

**INVESTIGATION OF THERMODYNAMIC PROPERTIES OF  
LIQUID BINARY ALLOYS**

**BY**

**ADEDIPE, ADEDAYO MAYOWA (B.Tech., FUTA)**

**(20144913688)**

**A THESIS SUBMITTED TO THE POSTGRADUATE SCHOOL,  
FEDERAL UNIVERSITY OF TECHNOLOGY,  
OWERRI**

**IN PARTIAL FULFILLMENT OF THE REQUIREMENTS  
FOR THE AWARD OF THE DEGREE OF MASTER  
OF SCIENCE (M.Sc.) IN PHYSICS**

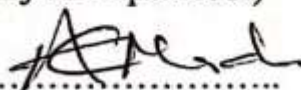
**NOVEMBER, 2019**

## CERTIFICATION

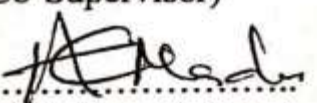
This is to certify that this research work entitled "Investigation of Thermodynamic Properties of Liquid Binary Alloys" was carried out by Adedipe Adedayo Mayowa (20144913688) in partial fulfilment of the requirement for the award of the Degree of M.Sc in Physics (Solid State Physics), in the Department of Physics, Federal University of Technology, Owerri.

  
.....  
Prof. I.C Ndukwe  
(Project Supervisor)

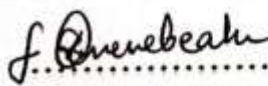
20/11/19.....  
Date

  
.....  
Prof. (Mrs) C.A Madu  
(Co-Supervisor)

22/11/2019.....  
Date

  
.....  
Prof. (Mrs) C.A Madu  
(Head of Department)

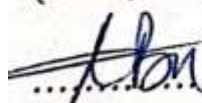
22/11/2019.....  
Date

  
.....  
Prof. C.C.Z Akaolisa  
(Dean, School of Physical Sciences)

22-11-19.....  
Date

.....  
Prof. (Mrs) Nnenna N. Oti  
(Dean, Postgraduate School)

.....  
Date

  
.....  
Prof. O.E Abumere ~~OS~~  
External Examiner

15/11/2019.....  
Date

## ACKNOWLEDGMENT

I am extremely grateful to my supervisors Professor I.C Ndukwe and Prof. (Mrs) C.A Madu for their assistance, guidance, and corrections. Special thanks to Dr. Y.A Odusote for providing materials on Fortran 95 and his assistance in programming the software. My deepest gratitude goes to Gbenga Oshakuade and my family for their effort, support, and prayer.

## TABLE OF CONTENTS

	<b>PAGES</b>
Title Page	i
Certification	ii
Dedication	iii
Acknowledgement	iv
Abstract	v
List of Figures	vi
List of Tables	vii
List of Appendices	viii
 <b>Chapter One</b>	
 <b>INTRODUCTION</b>	 1
1.1 Background to the research	1
1.1.1 Phase diagrams and thermodynamic properties	2
1.2 Research problem	3
1.3 Justification of the study	5
1.4 Scope of the study	6
1.5 Aim and objectives	7

## **Chapter Two**

LITERATURE REVIEW	8
2.1 Introduction	8
2.11 BiSb	8
2.12 BiSn	9
2.13 SbSn	9
2.2 Complex formation model and its two solution approximation	10
2.11 Conformal solution approximation	10
2.12 Flory's approximation	11
2.13 Concentration-concentration fluctuation	11
2.14 Warren-Cowley short range order parameter	12
2.3 Review on past research work	13

## **Chapter Three**

<b>METHODOLOGY</b>	27
3.1 Introduction	27
3.2 Gibbs free energy of mixing, $G_M/RT$	28
3.3 Concentration-concentration fluctuation	31
3.3 Warren-Cowley short range order parameter	33
3.4 Enthalpy and entropy of mixing	34

## **Chapter Four**

<b>RESULTS AND DISCUSSION</b>	35
4.1 Gibbs free energy of mixing, $G_M/RT$	35
4.2 Concentration-concentration fluctuations	38
4.3 Warren-Cowley Short-ranged order (SRO)	40
4.4 Enthalpy of mixing and entropy	43

## **Chapter Five**

<b>CONCLUSION</b>	48
5.1 Summary	48
5.2 Conclusion	51
5.3 Recommendation	53
5.4 Suggestion for further work	64
5.5 Contribution to knowledge	52 65
References	66
Appendix 1	56
Appendix 2	57
Appendix 3	58
Appendix 4	59
Appendix 5	60

## LIST OF FIGURES

PAGES

1. Figure 2.1. Concentration fluctuations  $S_{cc}(0)$  vs concentration. 16
2. (a) Tl-Te, (b) Mg-Bi, (c) Ag-Al, (d) Cu-Sn
3. Figure 2.2.  $G_M/RT$  vs concentration for Te-Ga liquid alloy at 1114K 17 and Te-Tl alloy at 1081K.
4. Figure 2.3.  $S_{cc}(0)$  vs concentration for Te-Ga liquid alloy at 1114K 19 and Te-Tl alloy at 1081K.
5. Figure 2.4. Calculated Warren-Cowley short range ordered  $\alpha_1$  versus 20 concentration for Te-Ga and Te-Tl liquid alloys
6. Figure 2.5.  $H_M/RT$  versus concentration for Te-Tl liquid 21 alloys at 1081k
7. Figure 2.6.  $S_M/RT$  versus concentration for Te-Tl liquid 21 alloys at 1081 k
8. Fig. 2.7. Concentration fluctuations in the long wavelength 22 limit  $S_{cc}(0)$  and  $S_{cc}^{id}(0)$  versus concentration for Cu-In liquid alloys at 1073 K
9. Figure 4.1. The graph of Gibbs free energy of mixing,  $G_M/RT$  33 versus concentration,  $C_{Bi}$  for Bi-Sb liquid alloy
10. Figure 4.2. The graph of Gibbs free energy of mixing,  $G_M/RT$  33 versus concentration,  $C_{Bi}$  for Bi-Sn liquid alloy
11. Figure 4.3. The graph of Gibbs free energy of mixing,  $G_M/RT$  34 Versus concentration,  $C_{Sn}$  for Sb-Sn liquid alloy
12. Figure 4.4. The graph of Concentration-concentration 35 fluctuation  $S_{cc}(0)$  versus Concentration,  $C_{Bi}$  for Bi-Sb liquid alloy.
13. Figure 4.5. The graph of Concentration-concentration 36 fluctuation,  $S_{cc}(0)$  versus Concentration, for Bi-Sn liquid alloy.
14. Figure 4.6. The graph of Concentration-concentration 36 fluctuation,  $S_{cc}(0)$  versus Concentration, for Sb-Sn liquid alloy.
15. Figure 4.7. The graph of Warren-Cowley Short ranged order 37 Parameter,  $\alpha_1$  versus Concentration,  $C_{Bi}$  for Bi-Sb liquid alloy.
16. Figure 4.8. The graph of Warren-Cowley Short ranged order 38 Parameter,  $\alpha_1$  versus Concentration,  $C_{Bi}$  for Bi-Sn liquid alloy.
17. Figure 4.9. The graph of Warren-Cowley Short ranged order 38 parameter,  $\alpha_1$  versus Concentration,  $C_{Sn}$  for Sb-Sn liquid alloy.

18.	Figure 4.10. The graph of Enthalpy of mixing $\frac{H_M}{RT}$ versus concentration, $C_{Bi}$ for Bi-Sb liquid alloy.	41
19.	Figure 4.11. The graph of Enthalpy of mixing $\frac{H_M}{RT}$ versus concentration, $C_{Bi}$ for Bi-Sn liquid alloy.	41
20.	Figure 4.12. The graph of Enthalpy of mixing: $\frac{H_M}{RT}$ versus concentration, $C_{Sn}$ for Sb-Sn liquid alloy.	42
21.	Figure 4.13. The graph of Entropy of mixing $\frac{S_M}{R}$ versus concentration, $C_{Bi}$ for Bi-Sb liquid alloy	43
22.	Figure 4.14. The graph of Entropy of mixing $\frac{S_M}{R}$ versus concentration, $C_{Bi}$ for Bi-Sn liquid alloy	43
23.	Figure 4.15. The graph of Entropy of mixing $\frac{S_M}{R}$ versus concentration, $C_{Sn}$ for Sb-Sn liquid alloy	44

## **LIST OF TABLES**

## **PAGES**

1. Table 2.1 Fitted values of the interaction parameters for liquid Te-Ga and Te-Tl alloys 17
  2. Table 4.1 Fitted values of the interaction parameters for Bi-Sb, Bi-Sn and Sb-Sn liquid alloys 32
  3. Table 4.2 Fitted values for temperature derivatives 40
- Interaction parameters for the Sb-Sn, Bi-Sb and Bi-Sn liquid alloys.

## **APPENDIX**

Appendix 1 : Symbols	54
Appendix 2: Calculated values of thermodynamics quantity Bi-Sb alloy at 1200k	55
Appendix 3: Calculated values of thermodynamics quantity Bi-Sn alloy at 600k	55
Appendix 4: Calculated values of thermodynamics quantity Sb-Sn alloy at 905k	56
Appendix 5: Program	57

## ABSTRACT

A complex formation model has been used to study the thermodynamic properties of Bi-Sb at 1200k, Bi-Sn at 905k and Sb-Sn at 600k binary liquid alloys. The research reveals that Bi-Sb and Sb-Sn alloys are weakly ordered systems and compound forming liquid alloys (hetero-coordinated) i.e., unlike atoms of Bi-Sb and Sb-Sn pairing as nearest neighbors, while Bi-Sn is not a compound forming alloy but exhibit phase segregation (homo-coordinated) i.e., like atoms of Bi-Sn pairing as nearest neighbors. The fitted and experimental values of the free energy of mixing of the three alloys compare well with each other at the temperature of interest. The value of  $g/RT$  (a measure of the formation of a complex in each alloy) in Bi-Sb and Sb-Sn are greater than zero, which shows that none of the two alloys has a strong tendency to form complexes, while the value for Bi-Sn is less than zero. The values of the Gibbs free energy of mixing,  $G_M/RT$  for Bi-Sb, Bi-Sn and Sb-Sn are found to be negative at all concentrations with a maximum value of -0.907, -0.640 and 0.926 respectively and are all symmetry at equiatomic composition (i.e  $c = 0.5$ ). The concentration-concentration fluctuation  $S_C(0)$  values for both Bi-Sb and Sb-Sn are less than the  $S_{CC}$  ideal ( $S_{cc}^{id}(0)$ ) values with a maximum value of 0.174 at  $c = 0.4$  and 0.172 at  $c = 0.5$  which justify that they are compound forming alloys. While BiSn  $S_C(0)$  exhibits a maximum value of 0.289 at  $c = 0.5$ , and greater than the ideal value and exhibited phase separation. Bi-Sb and Sb-Sn shows negative and minimum values for Warren-Cowley short-range order parameter  $\alpha_1$  as  $\alpha_1^{min} = -0.0391$  at  $c = 0.6$  and 0.0391 at  $c = 0.5$  respectively, these value is quite small compared to the value of  $\alpha_1$  for a complete ordering which is  $\alpha_1^{min} = -1.0$  and this implies a tendency towards clustering and indicates a weakly pronounced hetero-coordination. Bi-Sn exhibited a maximum value for Warren-Cowley shortrange order parameter  $\alpha_1$  as  $\alpha_1^{max} = 0.0680$ , this value is quite big compared to the value of  $\alpha_1$  for complete order which is  $\alpha_1^{min} = -1.0$ , this implies a high tendency towards segregation and indicates a strong pronounced homocoordination. In addition, it is observed that computed values and experimental values of this quantity are in very good agreement both in Bi-Sb, Bi-Sn and Sb-Sn alloys. From the thermodynamic properties, Bi-Sb and Sb-Sn are more suitable to be used as solders than Bi-Sn because they are compound forming alloys.

**Keywords:** Complex formation model, Binary liquid, BiSn, BiSb, SbSn .

# CHAPTER ONE

## INTRODUCTION

### 1.1 BACKGROUND TO THE RESEARCH

The development of the new lead-free solders has been a global trend due to environmental and health concerns for Pb toxicity (Chen *et al.*, 2016 ). Bi-based alloys can be substituted for conventional lead-tin solder because of their low melting point. Thermodynamic data are of great importance for the development of a new lead-free solder database, for the design of the new lead-free solder and for the prediction of various alloy properties (Glazer, 1995). In the last couple of decades, a substantial effort has been made to investigate the nature of atomic interactions of binary liquid alloys. The thermodynamic properties of such alloys deviate considerably from the ideal mixtures. Deviations could be positive or negative or both as a function of concentration  $C$ . It is believed that the deviations from ideal mixtures are artifacts of energetics and structural adjustment of competing complexes in the constituent element (Bhatia *et al.*, 1974). Theoretical models have been developed to investigate and explain the deviations or anomalies in terms of hetero-coordinated or homo-coordinated (segregation) binary alloy systems. Hetero-coordination is the preference of unlike atoms to pair together as nearest neighbours while segregation is the preference of like atoms to pair together as nearest

neighbours. From the viewpoint of theoretical modeling, the liquid binary alloys are broadly grouped into two major categories; symmetric and asymmetric alloys. Thermodynamic properties like Gibbs free energy of mixing  $G_M/RT$ , concentration-concentration fluctuations at long wavelength limit,  $S_{cc}(0)$ , Warren Cowley short range order parameter are symmetrical (Singh, 1987) or very close to it about concentration  $C = 0.5$ . These alloys are referred to as regular alloys. On the other hand the mixing properties of asymmetries alloys are not symmetrical about concentration  $C = 0.5$ . Great effort has been made to understand the cause of asymmetry and much attention has been focused on size effect or on the existence of chemical complexes in the liquid state.

### **1.1.1 PHASE DIAGRAMS AND THERMODYNAMIC PROPERTIES**

Thermodynamic properties of alloys include Gibbs free energy of mixing,  $G_M/RT$ , Heat of mixing  $\Delta H$ , Entropy of mixing  $\Delta S$ , Concentration-concentration fluctuations  $S_{cc}(0)$ , Warren-Cowley short-ranged order parameter. To understand the energetics of liquid binary alloys or obtain information about them, it is necessary to have a good understanding of phase diagrams and behavior of various thermodynamic properties. In a phase diagram, a liquidus line exhibits a defined peak at one or more concentrations which lie in the vicinity of the stoichiometric compositions of the binary liquid alloys (Singh, 1987). The thermodynamic properties of binary liquid alloys are found to have deviations (anomalies) around concentrations corresponding

to the peaks in the phase diagram. From the available phase diagram, one observes that Sb-Sn exhibits two intermetallic phases i.e the SbSn and  $Sb_2Sn_3$  in the Sb-Sn system (Jonsson and Agreen 1986). Comparing the Gibbs free energy of mixing of the two intermetallic phases (Arzpeyma *et al*, 2013), the SbSn phase is more stable than  $Sb_2Sn_3$ .

The basis for the choice of phase diagram adopted for the alloys in this study lies in the fact that available phase diagrams (Hultgren *et al.*, 1963) suggested that alloy could exhibit compound forming and segregation tendencies. A perusal of the phase diagrams (Asryan and Mikula, 2004) for Bi-Sb, Bi-Sn, and Sb-Sn show one of their individual stable complexes for Bi-Sb liquid alloy is BiSb, for Bi-Sn liquid alloy is BiSn and for Sb-Sn liquid alloy is SbSn.

## **1.2 RESEARCH PROBLEM**

Various methods have been used by many researchers which include complex formation models (Bhatia and Hargrove, 1974) to study thermodynamic properties of liquid binary alloys. Most of the previous research work by theorists on thermodynamic properties have been done using complex formation model or other available models to study the thermodynamic properties of binary alloys. In such model formulations, the deviation of the properties of the alloys from the ideal mixing conditions is discussed in terms of the interaction energies (which describes whether a like-atom pair or an unlike-atom pair is energetically preferred as the

nearest neighbour). It fails to provide information on Short-range order because the model ignores the extent of local ordering. Arising from the above, it follows that a major problem for choosing a thermodynamic alloy to work on is, how far do the liquid alloys thermodynamic properties deviate from the ideal properties. With respect to this deviation, an alloy can either be considered to be a compound forming (hetero-coordinated) liquid alloy or a segregating (homo-coordinated) system.

Such departures are visible as asymmetries in thermodynamic properties away from the equiatomic composition and usually ascribed to one of the following factors: size effect, electronegativity difference or the interaction between solute and solvent atoms. (Awe *et al.*, 2003).

The mixing behavior of such alloys, which is generally understood through the concentration-dependent thermodynamic properties, is greatly affected due to compound formation. The Gibbs free energy of mixing  $G_M/RT$ , of compoundforming liquid binary alloy deviates strongly from regular solution behavior and exhibits asymmetry around equiatomic concentration, ( $c=0.5$ ). Concentration fluctuation at long wavelength also exhibits maximum deviation from ideal solution values at compound-forming concentration.

Most of the previous research work by the theorists on thermodynamic properties have been model using Quasi-Chemical model (Anusionwu, 2006) to investigate thermodynamic and surface properties, Regular association solution model

(Adhikari, *et al.*,2011) to investigate concentration fluctuation in liquid magnesium alloy, and Ideal solution of Interaction product model (ISIP) (Kulikova, *et al.*, 2015). The majority of the existing models offer direct ways of properties calculation, which are complicated or even difficult to realize for a binary system. This study will focus on the investigation of thermodynamic properties using a Complex formation model to determine and explain the composition dependence of the thermodynamic properties of liquid alloys especially the ordering phenomena (concentration fluctuations in the long-wavelength limit and Warren-Cowley shortrange order parameter).

### **1.3 JUSTIFICATION FOR RESEARCH**

Alloys of Sn are very promising as an alternative solder in the electronics industry (Glazer, 1995). This is because the commonly used solder consists of lead which is known to be toxic to the human body and causes serious environmental problems (Chen et al., 2016). To develop a lead-free solder, a good knowledge of surface properties such as interfacial adhesion and surface tension is necessary. The thermodynamic model can be extended to investigate the composition dependence of surface tension and surface composition at the liquid-vapor interfaces of the liquid alloys. This is because these properties are known to play important role in the wettability and production of acceptable solder joint. In this research the thermodynamic properties of Bi-Sn, Bi-Sb and Sb-Sn are investigated with the aim

of determining and understanding from a theorist's point of view the properties of liquid binary alloys. To carry out this study and investigation, the complex formation model (Awe, et al 2003) which has proved successful in the study of thermodynamic properties and ordering in compound forming liquid alloys will be used to estimate and investigate the thermodynamic properties of alloys throughout the concentration range.

#### **1.4 SCOPE OF THE STUDY**

The research work will focus on the investigation of the thermodynamic properties of alloys using the Complex Formation Model.

Complex Formation Model has its basis on a distinctive aspect that molten mixtures, in their respective solid-state, form compounds at one or more definite compositions.

It is therefore assumed that in the molten state of the mixture there is a strong tendency for the two types of atoms to form a chemical complex  $A_\mu B_\nu$ .

CFM assumed that if the mixture of A and B atoms forms in the liquid state, there exists at a given temperature and pressure certain numbers of A and B atoms and chemical complex  $A_\mu B_\nu$  in chemical equilibrium with one another where  $\mu$  and  $\nu$  are assumed to be small integers.

It was assumed that a binary alloy consists of a pseudo ternary mixture of  $N_A = c$  moles of A atoms and  $N_B = N(1-c)$  moles of B atoms, and a type  $A_\mu B_\nu$  of the

chemical complex. Here  $\mu$  and  $\square$  are assumed to be small integers,  $c$  is the atomic fraction of A atoms and  $N$  is the Avogadro's number.

which has its basis on a distinctive aspect that molten mixtures, in their respective solid-state, form compounds at one or more definite compositions. The model can be applied to two higher approximation approaches namely; Conformal solution approach and Flory's solution approximation. In this research work Flory's approximation approach will be used to determine bulk thermodynamic properties such as concentration-concentration fluctuation at long-wavelength limit, WarrenCowley short-range order parameter, enthalpy, and entropy of mixin, but the research work will not cover thermodynamic surface properties (surface tension and surface segregation) and transport properties (diffusivity and viscosity).

### **1.5 AIM AND OBJECTIVES**

The aim of the research is to investigate the composition dependence of various thermodynamic properties such as Gibbs free energy of mixing, concentrationconcentration at long wavelength  $S_{cc}(0)$ , thermodynamic activity  $\alpha_1$ , short-range order, enthalpy of mixing and entropy of chosen liquid binary alloys on concentration. The objectives are:

1. To analyze the compound formation phenomenon in Bi-Sb (Bismuth antimony),

Bi-Sn (Bismuth tin) and Sb-Sn (Antimony tin) liquid alloy systems at temperatures 1200K, 600K and 905K respectively through the study of their thermodynamic properties.

2. To investigate the noticeable departure or deviation from ideal mixing condition in the relevant thermodynamic properties in terms of the interaction energies of the constituent system of the respective alloys.

## **CHAPTER TWO**

### **LITERATURE REVIEW**

#### **2.1 INTRODUCTION**

The complex formation model was first used (Bhatia and Hargrove, 1974) to investigate concentration fluctuations and the thermodynamic properties of some compounds forming binary molten systems. This chapter will discuss the complex formation model two higher solution approximations and review some related past research work.

##### **2.1.1 BiSb**

BiSb alloys are interesting from the physics point of view because they can exhibit semimetallic, semiconductor, or metallic characteristics, depending on the percentage of Sb, and temperature (Ibrahim and Thompson, 1985). However, the addition of Sb can lead to a positive energy gap and the formation of solid solution leads to a reduction in the lattice thermal conductivity. Bismuth and Antimony both belong to group 15 and both have a face-centered rhombohedra crystal structure, with Bismuth having an atomic number of 83 and period 6, while Antimony has the atomic number of 51 and period 6. The BiSb alloys are promising not only because of the particular interest for low-temperature thermoelectric industry and refrigeration or the interesting physical properties but also for their interest as engineering materials. The structure of their conduction and valence band strongly

depends on various parameters such as alloy composition, temperature, external pressure and magnetic field (Lenoir et al., 1996) Bi-Sb alloys are still the best n-type materials for refrigeration at low temperature.

### **2.1.2 BiSn**

BiSn alloys are candidates for consumer products with low operating temperature and for temperature-sensitive components and substrates. It is a simple eutectic system. Bismuth and Tin both belong to groups 15 and 14 respectively, with Bismuth having atomic number of 83 and period 6, while Tin has the atomic number 50 and period 5.

### **2.1.3 SbSn**

Soldering is the most important for soldering in the electronics industry. An alloy of Sn is very promising as an alternative solder in the electronics industry (Glazer, 1995). This is because the commonly used solder consists of lead which is known to be toxic to the human body and causes a serious environmental problem (Chen et al., 2016). Progress has been made in the area of low-temperature lead-free solders while the research is lacking in replacing high-temperature Pb-Sn solder alloys. Sb-Sn alloys are considered as a candidate among the high-temperature solder alloys such as Au-Sn, Au-Ge, Ag–Bi-Sn, It exhibits good electrical properties and a wide range of melting temperatures that make them applicable in stepsoldering technology (Novakovic et al., 2011). To develop a lead-free solder, a good

knowledge of surface properties such as interfacial adhesion, surface tension (Anusionwu., 2006) and bulk properties is necessary.

Antimony and Tin both belong to period 5 and groups 15 and 14 respectively, Tin with an atomic number of 50, while Antimony has atomic number of 51.

### **2.2.1 Conformal solution approximation**

This is sometimes referred to as regular solution in the zeroth approximation and generally considered to be reasonable or valid when the effect of the differences in sizes of the various constituents in the mixture can be ignored and the differences in the interactions between different species are zero (Bhatia and Hargroove 1974)

$$\Delta G = RT \sum n_i \ln \left( \frac{n_i}{n} \right) + \sum_{i<j} \sum \frac{n_i n_j}{n} w_{ij} \quad (2.1)$$

Equation (2.1) is referred to as a conformal approximation solution. Therefore the free energy of mixing  $G_M$  for the compound forming alloy in conformal solution approach using the expression in Equation (2.1) is given as

$$G_M = -n_3 g + RT \sum_{i=1}^3 n_i \ln \left( \frac{n_i}{n} \right) + \sum_{i<j} \sum \frac{n_i n_j}{n} w_{ij} \quad (2.2)$$

Where  $w_{ij}$  ( $\equiv 0$  for  $i = j$ ) are the interaction energies.

### **2.2.2 Flory's solution approximation**

The effect of differences in sizes between A, B and  $\mu B_v$  are very difficult to take into account, but due to the work of Flory in polymer physics (Flory, 1942), the differences in size and interaction energies are well treated (Bhatia and Hargrove 1974). The expression for the free energy of mixing is given as follows;

$$\Delta G = RT \left[ \sum_{i=1}^2 n_i \ln \left( \frac{n_i}{N} \right) + n_3 \ln \left\{ \frac{(\mu+v)n_3}{N} \right\} + \sum_{i<j} \sum \left\{ \left( \frac{n_i n_j}{N} \right) \frac{v_{ij}}{RT} \right\} \right] \quad (2.3)$$

Equation (2.3) is referred to as Flory's approximation solution. Using the expression in Equation (2.3) the free energy of mixing  $G_M$  for the compound forming alloy in Flory's solution approximation is given as

$$G_M = -n_3 g + RT \left[ \sum_{i=1}^2 n_i \ln \left( \frac{n_i}{N} \right) + n_3 \ln \left\{ \frac{(\mu+v)n_3}{N} \right\} + \sum_{i<j} \sum \left\{ \left( \frac{n_i n_j}{N} \right) \frac{v_{ij}}{RT} \right\} \right] \quad (2.4)$$

### **2.2.3 Concentration-concentration fluctuation ( $S_c(0)$ )**

An important parameter in studying the nature of ordering in liquid binary alloys is the long-wavelength limit of the concentration-concentration fluctuation  $S_c(0)$ , which has emerged as an important function to understand alloying behavior in terms of compound formation and phase segregation.  $S_c(0)$  is thermodynamically related to the free energy of mixing,  $G_M$  and activity,  $\alpha_A$ .

$$\begin{aligned} S_{CC}(0) &= \frac{NK_B T}{\left( \frac{\partial^2 G_M}{\partial c^2} \right)_{T,P,N}} = RT \left( \frac{\partial^2 G_M}{\partial c^2} \right)_{T,P,N}^{-1} = (1-c) \alpha_A \left( \frac{\partial \alpha_A}{\partial c} \right)_{T,P,N}^{-1} \\ &= c \alpha_B \left[ \frac{\partial \alpha_B}{\partial (1-c)} \right]_{T,P,N}^{-1} \end{aligned} \quad (2.5)$$

In the above equation  $\alpha_A$  and  $\alpha_B$  are thermodynamic activities of components A and B in the mixture. It may be emphasized that  $\left( \frac{\partial^2 G_M}{\partial c^2} \right)$  is also known as the stability of the solution. The reciprocal of  $S_c(0)$ , i.e.  $RT / S_{CC}(0)$ , is a measure of the stability of the mixture

$S_c(0)$  can also be derive in terms of  $n_i$ , its derivatives with respect to concentration,

$v_{ij}$  and its coordination number  $Z$ ; therefore,

$$S_C(0)^{-1} = \Lambda + Y \quad (2.6)$$

Where

$$\Lambda = \left( \sum_{i=1}^3 \frac{(n_i)^2}{n_i} \right) - \frac{\frac{1}{2} Z \delta^2 (n'_3)^2}{\Phi} \quad (2.7)$$

and

$$Y = \frac{2}{\Phi_{RT}} \sum \sum_{i < j} v_{ij} \left( n'_i n'_j + \frac{\partial n'_3 (n'_i n'_j + n_i n'_j)}{\Phi} \right) + \frac{\partial^2 (n'_3)^2 n_i n_j}{\Phi} \quad (2.8)$$

The prime on the n's refers to their first derivative with respect to c (Akinlade et al., 2000).

#### **2.2.4 Warren-Cowley short-range order ( $\alpha_i$ )**

For an alloy consisting of A and B atoms, in the proportions of  $m_A$  and  $m_B$ , shortrange order parameter will be defined for the atomic site with coordinates l,m,n with respect to a given B atom as  $\alpha_{lmn} = 1 - p_{lmn}/m_A$  where  $p_{lmn}$  is the probability that the atomic site is occupied by an A atom. Therefore,

$$p_{lmn} = m(1 - \alpha_{lmn}) \quad (2.9)$$

If an A atom is taken as origin,

$$p_{lmn} = m_A + m_B \alpha_{lmn}. \quad (2.10)$$

Alternatively, if the atom with coordinates l,m,n is considered to belong to the  $i$ th shell of neighbors surrounding a B atom, then  $\alpha_i = 1 - n_i/m_{AC_i}$ , where  $n_i$  is the number of A atoms among the  $c_i$  atoms of the  $i$ th shell. The conversion properties of order parameters are that they are zero for the complete random state, and have a maximum (absolute) value for perfect order. The value for perfect order  $\alpha_i$ , is unity (Cowley, 1950).

### **2.3 Review on some of the other related work**

The complex formation model has found popular use in the study of thermodynamic properties of liquid binary alloys. CFM was used to investigate thermodynamic properties of some compound forming binary molten systems (TiTe, Mg-Bi, Ag-Al, and Cu-Sn), where the concentration dependence of the free energy of mixing  $G_M$ , activities  $\alpha_1$ , concentration fluctuations  $S_{CC}(0)$  at long wavelength, enthalpy and entropy of mixing were studied.

The four liquid binary alloys were treated with two higher approximations so as to compare the results with the existing experimental data (a) in the conformal solution approximation and (b) in Flory's approximation, solving the above equations numerically, value for Gibbs free energy of mixing was obtained. Having obtained the Gibbs free energy of mixing, other thermodynamic functions, which are related to  $G_M$  through thermodynamic relation was obtained, such as activity  $\alpha_A$ , Warren-Cowley short-range order parameter and concentration-concentration fluctuations

$S_C(0)$ .

CFM and its basic assumptions were used. The fundamental assumptions of the complex formation model are that a compound forming binary AB alloy in the liquid state consists of  $n_1$  individual A atoms,  $n_2$  individual B atoms and  $n_3$  complexes of

the type  $A_\mu B_\nu$  all in chemical equilibrium.  $\mu$  and  $\nu$  are small integers numbers. The atoms are supposed to be located on lattice sites and have  $z$  nearest neighbors. Given that the total number of lattice sites is just  $N$ , It follows that:

$$n_1 = Nc - \mu n_3, \quad n_2 = (1 - c) - \nu n_3, \quad (2.11)$$

where  $c$  is the concentration of A atoms.

and

$$n = n_1 + n_2 + n_3 = N - (\mu + \nu - 1)n_3. \quad (2.12)$$

The Gibbs free energy of mixing of the binary alloy can be expressed as

$$G_M = -n_3 g + \Delta G \quad (2.13)$$

In this equation,  $g$  is the formation energy of the complex and the term  $-n_3 g$  represents the lowering of the free energy due to the formation of complexes in the alloy.  $\Delta G$  represents the free energy of mixing of the ternary mixture of fixed  $n_1$ ,  $n_2$ , and  $n_3$  whose constituents A, B and  $A_\mu$  are assumed to be interacting weakly with each other. The strong bonding interaction between the individual elements A and B have been taken into account via the formation of the chemical complex. The Flory solution approximation was then introduced (using equation 2.3) so as to compute  $n_3$  and  $G_M$  (Our work will be modeled using this exact solution approximation in Chapter 3). Using  $\Delta G$  as originally formulated by Flory (Lingley et al., 2011).

The free energy of mixing (by Flory approximation) was obtained by combining Eq. (2.3) and (2.4) as

$$G_M = -n_3 g + RT \left[ \sum_{i=1}^2 n_i \ln \left( \frac{n_i}{N} \right) + n_3 \ln \left\{ \frac{(\mu + \nu)n_3}{N} \right\} + \sum_{i < j} \sum \left\{ \left( \frac{n_i n_j}{N} \right) \frac{v_{ij}}{RT} \right\} \right] \quad (2.14)$$

Here, R is the molar gas constant, the  $V_{ij}$ 's ( $i, j = 1, 2, 3$ ) are the interaction energies through which A, B, and AB interact with one another, and by definition, independent of composition although they may depend on temperature and pressure.

The equilibrium value of  $n_3$  at a given temperature and pressure is given by

$$\left(\frac{\partial G_M}{\partial n_3}\right)_{T,P,N,c} = 0 \quad (2.15)$$

From Equation (2.15) and Eq. (2.14) the equilibrium values of  $n_3$  was given by solving Eq. (2.16) obtained after differentiating Eq. (2.14) with respect to  $n_3$  and rearrangement of terms using Eq. (2.5).

$$n_1^\mu n_2^\nu = (n_3 N^{\mu+\nu-1}) K e^Y \quad (2.16) \text{ where}$$

$$K = \exp\left(\frac{-g}{RT}\right), \quad \text{and}$$

$$Y = \frac{1}{nRT} \left[ v_{12} \left( Y \frac{n_1 n_2}{n} - \mu n_2 - \nu n_1 \right) + v_{13} \left( Y \frac{n_1 n_3}{n} - \mu n_3 + n_1 \right) + v_{23} \left( Y \frac{n_2 n_3}{n} - \nu n_3 + n_2 \right) \right] \quad (2.17)$$

Eqs. (2.16). was solved numerically to obtain equilibrium values of  $n_i$  ( $i = 1, 2, 3$ ) for given energy parameters  $g$  and  $v_{ij}$ . Having obtained the free energy of mixing, the thermodynamic activities was obtained using the general relationship in Eq. 2.18

$$RT \ln \alpha_X = \left(\frac{\partial G_M}{\partial N_X}\right)_{T,P,N} \quad (2.18)$$

In the equation (2.18), X refers to the components of A or B from which one can write

$$\ln \alpha_A = \ln \left(\frac{n_1}{N}\right) + \frac{1}{RT} \left[ \left(\frac{n_2}{n}\right) V_{12} + \left(\frac{n_3}{n}\right) V_{13} - \sum \sum_{i>j} \left(\frac{n_i}{n}\right) \left(\frac{n_j}{n}\right) V_{ij} \right] \quad (2.19)$$

and

$$\ln \alpha_B = \ln \left(\frac{n_2}{N}\right) + \frac{1}{RT} \left[ \left(\frac{n_2}{n}\right) V_{12} + \left(\frac{n_3}{n}\right) V_{23} - \sum \sum_{i>j} \left(\frac{n_i}{n}\right) \left(\frac{n_j}{n}\right) V_{ij} \right] \quad (2.20)$$

In order to use the complex formation model, the values of the interaction parameters  $g$  and  $w_{ij}$  were fitted in such a way that the values obtained yielded the

least deviation between experimental and fitted values of the Gibbs free energy of mixing

$G_M$ .

The concentration-concentration fluctuation in the long-wavelength limit,  $S_C(0)$  is thermodynamically related to the free energy of mixing,  $G_M$  and thermodynamic activity  $\alpha_A$ . The relationship between  $S_C(0)$  and  $G_M$  is giving by

$$S_{CC}(0) = RT \left( \frac{\partial^2 G_M}{\partial C^2} \right)_{T,P,N}^{-1} = (1 - C) \alpha_A \left( \frac{\partial \alpha_A}{\partial C} \right)_{T,P,N}^{-1} = c \alpha_B \left[ \frac{\partial \alpha_B}{\partial (1-c)} \right]_{T,P,N}^{-1} \quad (2.21)$$

In equation 2.21,  $\alpha_A$  and  $\alpha_B$  are thermodynamic activities of components A and B in the mixture. Once the Gibbs energy of mixing has been fitted, all the parameters required for the calculation of  $S_C(0)$  must have been determined and are kept constant during the course of the calculations. The basic rule is that when  $S_C(0) \ll$

$S_{CC}^{id}(0)$  i.e., computed values are less than the ideal values, it implies a tendency for heterocoordination (preference for unlike atoms to pair at nearest neighbours) while when  $S_{CC}(0) \gg S_{CC}^{id}(0)$  indicates a tendency for homo-coordination, a phase segregation (preference for like atoms to pair as the nearest neighbor).

In order to measure the degree of order in the liquid alloy, the Warren-Cowley shortrange order parameter  $\alpha_1$  was computed. Experimentally,  $\alpha_1$  can be determined from knowledge of the concentration-concentration  $S_C(q)$  and number-number structure factors  $S_{NN}(q)$ . However, in most diffraction experiments, these quantities are not easily measurable. On the other hand,  $\alpha_1$  can be estimated from knowledge of  $S_C(0)$  using the equation (2.16). When  $\alpha_1 = 0$  correspond to a random distribution of atoms, while  $\alpha_1 < 0$  refers to unlike atoms pairing as nearest neighbors whereas  $\alpha_1 > 0$  corresponds to a situation in which like atoms pair in the first coordination shell. For equiatomic composition the limiting values of  $\alpha_1$  lie in the range  $-1 \leq \alpha_1$

$\leq +1$  and the minimum value of  $\alpha_1$  is  $\alpha_1^{minimum} = -1$ , implying a complete ordering of unlike atoms as nearest neighbors. On the other hand, the maximum value  $\alpha_1^{maximum} = 1$  implies total segregation leading to phase separation.  $\alpha_1$  can be computed from  $S_c(0)$ :

$$\alpha_1 = \frac{s-1}{s(z-1)+1}, \quad S = \frac{S_{cc}(0)}{c(1-c)} \quad (2.22)$$

$z$  being the coordination number of the alloy is taken as 12 while  $S_{cc}(0)$  values are obtained from Eq. (2.21).

With regard to other bulk thermodynamic properties, the calculation of enthalpy and entropy of formation are of great importance because they provide information on the temperature dependence of the interaction parameters. When the temperature dependence of the interaction parameter was neglected and both  $H_M$  and  $S_M$  is computed. It was observed that the computed values of these quantities deviate significantly from the experimental values and significant improvements could only be obtained when the temperature dependence of the interaction parameters was incorporated. The enthalpy of formation,  $H_M$ , was obtained from the standard thermodynamic expression.

$$H_M = G_M - T \left( \frac{\partial G_M}{\partial T} \right)_P \quad (2.23)$$

Expression for  $G_M$  was substituted in Eq. (2.23) to obtain

$$H_M = -n_3 \left( g - T \frac{\partial g}{\partial T} \right) + \sum_{i < j} \sum n_i n_j \left( V_{ij} - T \frac{\partial V_{ij}}{\partial T} \right) \quad (2.24)$$

and the Entropy of mixing  $S_M$

$$S_M = \frac{H_M - G_M}{T} \quad (2.25)$$

From the expression for  $G_M$  in Eq. (2.14) and expression of  $H_M$  in Equation (2.24) expression for  $S_M$  using Eq. (2.25) was obtained as

$$S_M = -n \left( \frac{\partial g}{\partial T} \right)_p - R [n_1 \ln n_1 + n_2 \ln n_2 + n_3 \ln \{(\mu + \nu)n_3\}] - \sum_{i < j} n_i n_j \left( \frac{\partial v_{ij}}{\partial T} \right)_p \quad (2.26)$$

For two of the molten systems considered namely Mg-Bi and Tl-Te which in the solid-state form are highly stable compounds  $Mg_3Bi_2$  ( $\mu = 3, \nu = 2$ ) and  $Tl_2Te$  ( $\mu = 2, \nu = 1$ ),  $|G(c_c)/NRT| > 3$  at the temperature of observation. At the chemical

composition  $c_c = \frac{\mu}{(\mu + \nu)}$ , It was discovered that the composition for system

c to be less than 0.001, in which one of the interaction parameter  $w_{12}$  could not be determined from the experimental data on  $G_M$ . For the other two systems considered, Ag-Al and Cu-Sn, which were assumed to form chemical complexes

$Ag_3Al$  ( $\mu = 3, \nu = 1$ ) and  $Cu_4Sn$  ( $\mu = 4, \nu = 1$ ), respectively,  $|G_M/NRT| \cong 1.2$  and

0.9 at respective chemical composition. This implies smaller values of  $|G_M/NRT|$

(larger K or weaker tendency to form chemical complexes) than for Mg-Bi and TlTe.

It was observed that the tendency of compound formation in Mg-Bi and Tl-Te is greater than that of the Ag-Al and Cu-Sn system. It is observed that in Tl-Te liquid alloy,  $S_{cc}(0)^{cal} < S_{cc}(0)^{ideal}$ , that is, in the region  $0 \leq C_{Tl} \leq 0.7$  there is

heterocoordination while in the region  $0.7 \leq C_{Tl} \leq 1.0$   $S_{cc}(0)^{ideal} < S_{cc}(0)^{calculated}$

which implies self-coordination that lead to phase segregation, while in Cu-Sn

$S_c(0)^{cal} < S_{cc}(0)^{ideal}$  at all composition, indicates a tendency for heterocoordination

(preference for unlike atoms to pair at nearest neighbours). (Bhatia and Hargrove.,1974).

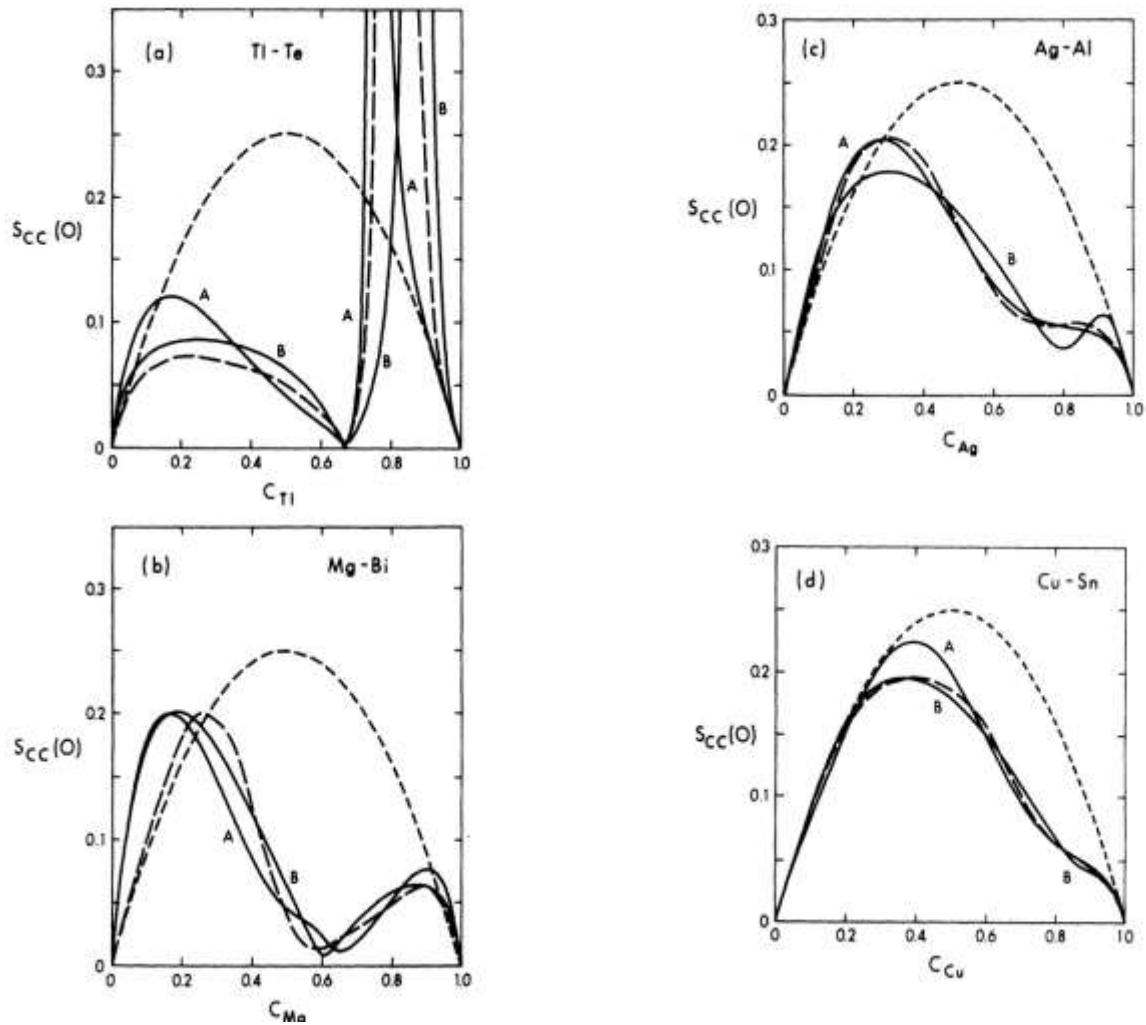


Fig. 2.1. Concentration fluctuations  $S_{CC}(0)$  vs concentration. (a) Tl-Te, (b) Mg-Bi, (c) Ag-Al, (d) Cu-Sn. (Bhatia and Hargrove.,1974.).

However, from the reviewed literature, CFM has been useful in investigating thermodynamic properties of liquid alloys that exhibited ordered-disorder transformation (compound forming to phase-segregation) as in Te-Ga and Te-Tl, Flory's approximation solution approach was adopted and by following the same

steps and approach, from equations (2.14) and (2.15) the values of  $n_3$  for the two liquid alloys was obtained by the solution of Eq. (2.10). Numerical solution of Eq. (2.16) provides equilibrium values of  $n_3$  which was used to obtain  $G_M$  from Equation (2.4). The values of  $g$  and  $V_{ij}$  for the Te-Ga and Te-Tl liquid alloys being investigated are given in Table 2.1.

Table 2.1

Fitted values of the interaction parameters for the liquid Te-Ga and Te-Tl alloys (Awe et al., 2003)

System	$g/RT$	Temp/K	$V_{12}/RT$	$V_{13}/RT$	$V_{23}/RT$
Te-Ga	2.2	1114	9.0	-1.3	2.6
Te-Tl	3.1	1081	-0.98	2.74	-0.3

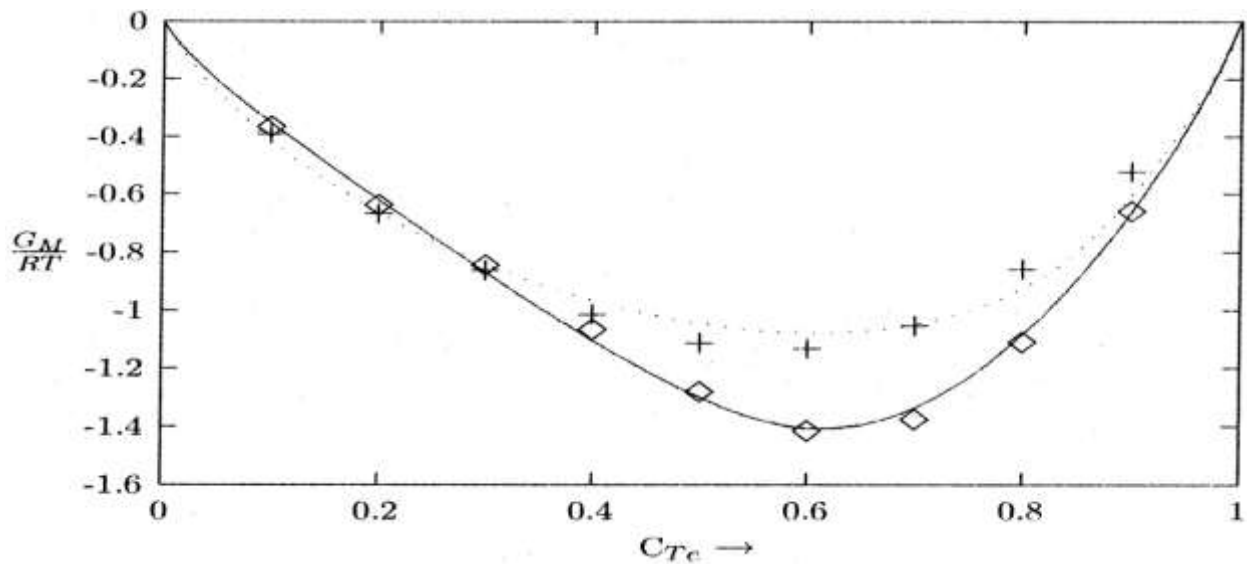


Fig. 2.2.  $G_M/RT$  vs Concentration for Te-Ga liquid alloy at 1114K and Te-Tl alloy at 1081K. Diamond symbol represents experimental values for Te-Ga, crosses are

for Te-Tl, solid lines are the calculated values for Te-Ga and dots are for Te-Tl. (Awe et al., 2003)

It was concluded (Awe et al., 2003) that, since the fitted and experimental values of the free energy of mixing compare well with each other, it shows that the fitted values of the interaction parameters for the two systems, Te-Ga and Te-Tl are quite good at the temperature of interest as shown in Fig. 2.2. From the point of view of the four interaction parameter, that is,  $g$  and  $V_{ij}$ , the latter is the most physically meaningful since it is a measure of the formation of the complex in each alloy. Although the value of  $g/RT$  in each of the two liquid alloys is greater than zero, yet the fact that the value is low in each of them justifies the conclusion that none of the two alloys has a strong tendency to form complexes. In other words, a low value of  $g/RT$  in each of the two systems confirms that they are weakly interacting systems. With regard to the other interaction parameters,  $V_{12}$ ,  $V_{13}$ , and  $V_{23}$ , explaining their physical meaning using a scheme in which subscript 1 represents the A atoms, 2 represent B atoms and 3, the complex  $A_\mu B_\nu$ .  $V_{12}$  is a measure of the interaction between A and B atoms. Thus, a positive value of the parameter is indicative of an alloy that exhibits homo-coordination at certain compositions, while a negative value is evidence of a hetero-coordinated system. This is evident from Table 2.1, for Te-Ga which has a positive value of  $V_{12}$ ; it undergoes a transition from phase separating to an ordered while Te-Tl exhibits compound formation throughout the whole composition range.

By making use of the values of interaction parameters shown in the table above for each of the two systems, Eq. (2.17) was used to obtain numerical values of  $n_1$  and  $n_2$  via Eq. (2.11). The value of the interaction parameter as shown in Table 2.1 were then put in Eq. (2.20) to calculate thermodynamic activity for each of the two systems.

The concentration-concentration fluctuation in the long-wavelength limit,  $S_{CC}(0)$  was determined (Awe et al., 2003) and Fig. 2.3 shows the comparison of experimental and calculated values of this quantity for the two liquid alloys. There is a relatively good agreement between experimental and calculated values of  $S_C(0)$ . It was observed from their work (Awe et al., 2003) that in Te-Ga liquid alloy,

$S_{CC}(0)^{calculated} > S_{CC}(0)^{ideal}$ , that is, in the range  $0 \leq C_{Te} \leq 0.480$  there is selfcoordination which will lead to phase segregation while in the region  $0.480 \leq C_{Te}$

$\leq$

1.0.  $S_C(0)^{ideal} > S_{CC}(0)^{calculated}$  which implies hetero-coordination.

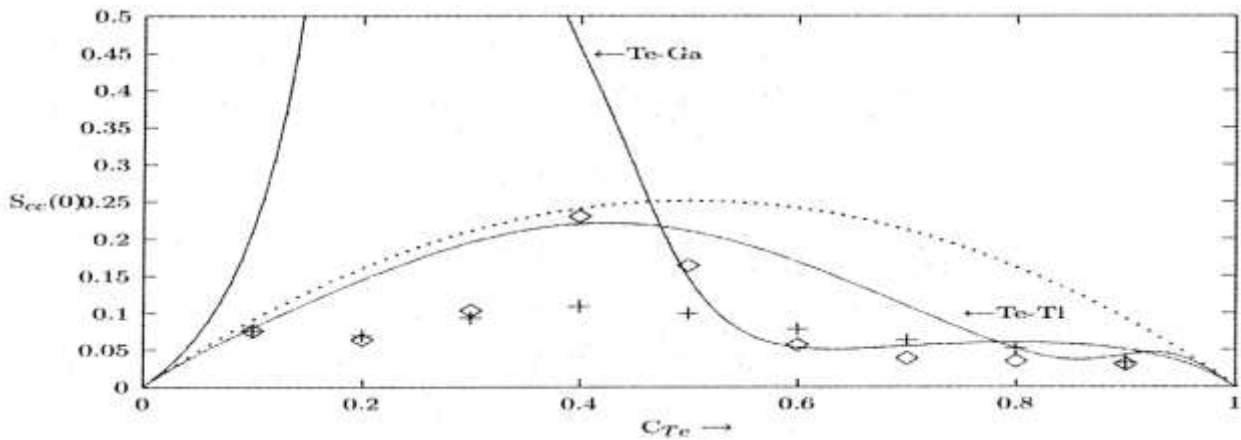


Fig. 2.3  $S_C(0)$  versus concentration for Te-Ga and Te-Tl liquid alloys. The diamond symbol is experimental values for Te-Ga, crosses are for Te-Tl, the dots represent the ideal values, In both cases, solid lines are the calculated values.(Awe et al., 2003)

Warren-Cowley short-range order parameter was computed for the liquid alloys as well so as to measure the degree of order in the liquid alloy, it was observed from the investigation (Awe et al., 2003) that  $\alpha_1$  is negative at all composition in Te-Tl alloy (Fig. 2.4.) and that Te-Tl is a compound forming liquid alloy over the whole

composition range. Unlike Te-Tl,  $\alpha_1$  for Te-Ga reveals that within the concentration range  $0.0 \leq C_{Te} \leq 0.480$  Te-Ga is weakly ordered because  $\alpha_1 < 0$ . Also  $\alpha_1$  of Te-Ga shows that within the remaining range of concentration (i.e  $0.480 \leq C_{Te} \leq 1.0$ ) it is chemically ordered.

It was thereby, concluded (Awe et al., 2003) that Te-Ga exhibited order-disordered transformation while Te-Tl exhibits compound forming throughout the composition range, and at a temperature of 1081K, the alloy Te-Tl is chemically ordered and that the most likely clustered which exist in the melt is  $Tl_4Te$ . At a temperature of 1114K, the Te-Ga liquid alloys display an ordered-disorder transformation (compound forming to phase-segregation) (Awe et al., 2003).

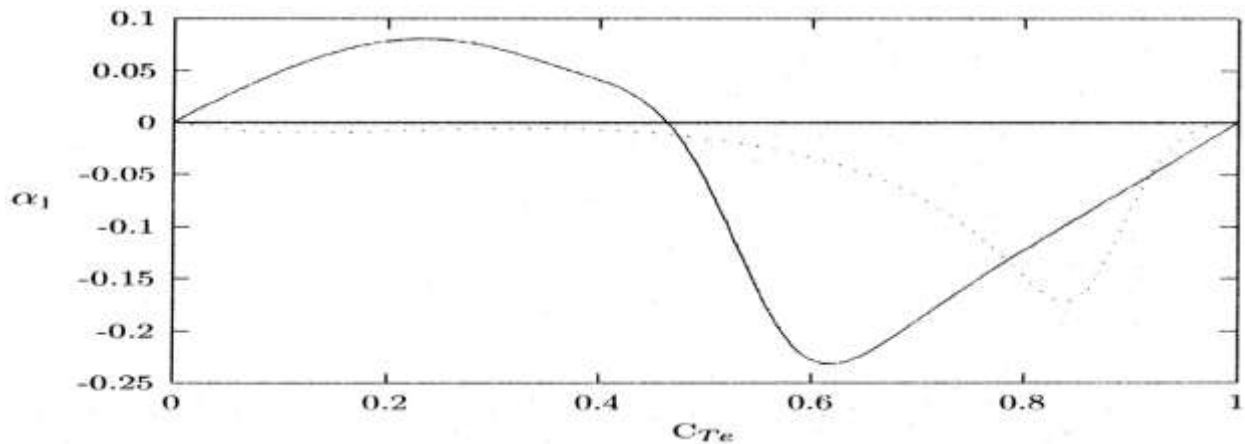


Fig 2.4 Calculated Warren-Cowley short-range ordered  $\alpha_1$  versus concentration for Te-Ga (solid lines) and Te-Tl (dotted lines) liquid alloys. (Awe et al., 2003)

It was reported (Awe et al., 2003) that in Te-Ga and Te-Tl liquid alloys, the fitted  $H_M/RT$  and resulting  $S_M/RT$  as shown in Fig. 2.5 and 2.6, are in good agreement with the experimental except some deviation in  $S_M/RT$ .

Fig. 2.6 shows that there is an excellent agreement between the experimental values of  $S_M$  for the Te-Tl system. The fact that  $S_M/R$  quantity is negative throughout the

whole composition confirms again that Te-Tl at 1081K is chemically ordered throughout the whole composition.

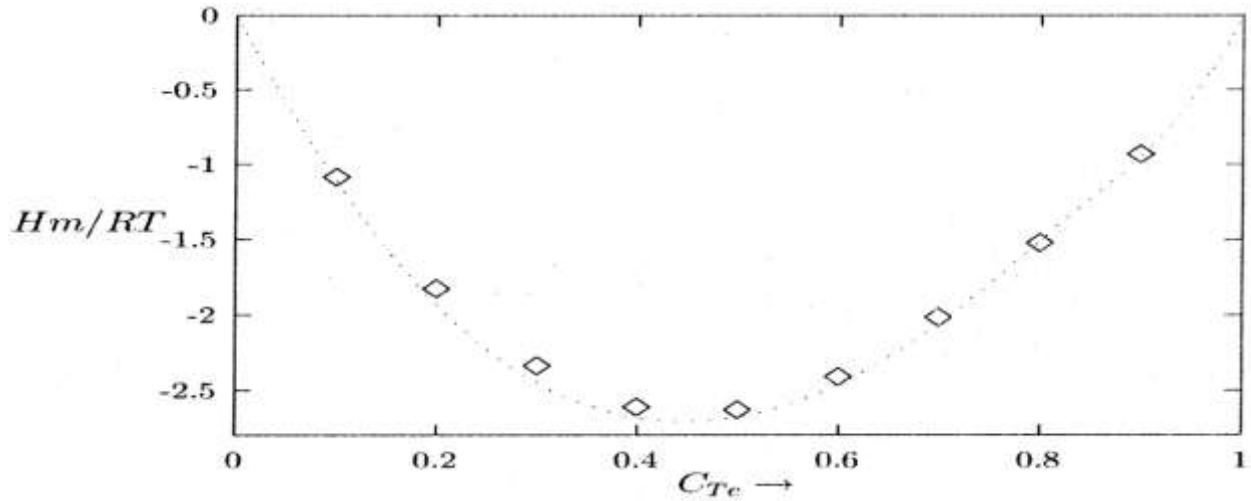


Fig. 2.5  $H_m/RT$  versus concentration for Te-Tl liquid alloys at 1081 k. The dots represent calculated values while the diamond symbol represents experimental values. (Awe et al., 2003)

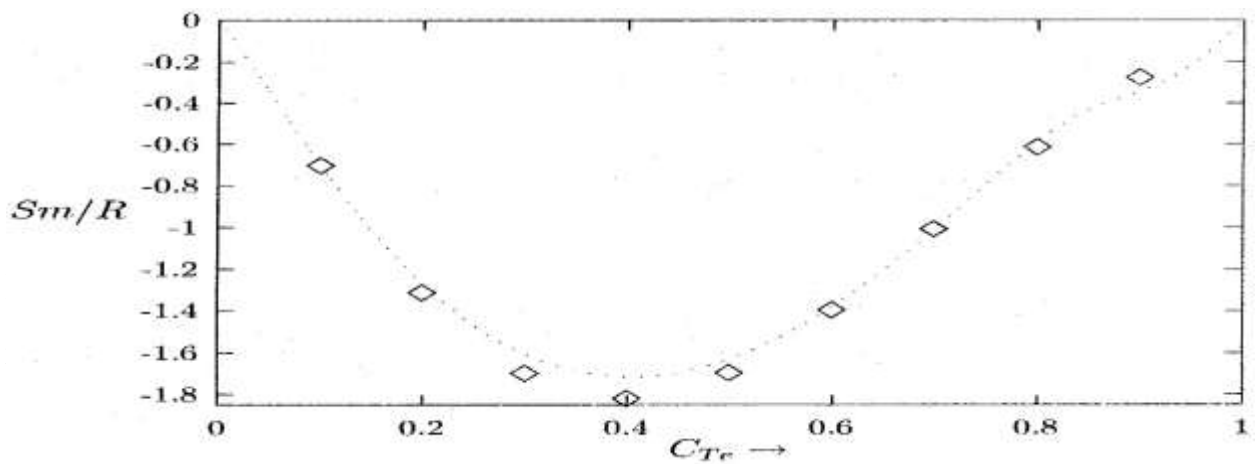


Fig. 2.6  $S_m/R$  versus concentration for Te-Tl liquid alloys at 1081 k. The dots represent calculated values while the diamond symbol represents experimental values. (Awe et al., 2003)

Moreover, a complex formation model by way of Flory approximation was also used to study Cu in molten Cu-In alloys. Using the same approach as the reviews (Awe et al., 2003) above, a complex formation model that assumes the existence of  $\text{CuIn}_4$  compound in Cu-In liquid alloy was satisfactorily used to obtain the parameters, which fit the experimental  $G_M/RT$  values for the Cu-In alloy. The concentrationdependence of their various thermodynamic properties has been discussed. The fitted parameters were used to compute  $S_{cc}(0)$ , the Warren-Cowley short-range parameter and diffusion coefficient, and it was deduced that Cu-In alloy undergoes a transformation from an ordered state to a segregated state.

It was observed (Awe et al., 2003) from Fig. 2.7, that the computed  $S_{cc}(0) < S_{cc}^{id}(0)$  in the composition range,  $0 \leq c_{Cu} \leq 0.5$ , indicates a tendency for heterocoordination, i.e., unlike atoms Cu–In pairing as nearest neighbors, whereas in the composition range  $0.5 \leq c_{Cu} \leq 1.0$ , there is tendency for homo-coordination,  $S_{cc}(0) > S_{cc}^{id}(0)$ , i.e., like atoms Cu–Cu tend to pair as nearest neighbors. In addition, the phenomenon of easy glass formation was predicted and interpreted by the knowledge of the concentration–concentration fluctuations in the long-wavelength limit,  $S_{cc}(0)$ . The concentration range where the difference  $|S_{cc}^{id}(0) - S_{cc}(0)|$  tends to zero may be considered as a necessary condition for glass formation. In the Cu-rich end region ( $c_{Cu} > 0.80$ ) of the Cu–In system, the calculated  $S_{cc}(0)$  values are close to the ideal values,  $S_{cc}(0) \approx S_{cc}^{id}(0)$ , supporting the glass formation tendency in the system.

(Odusote., 2008).

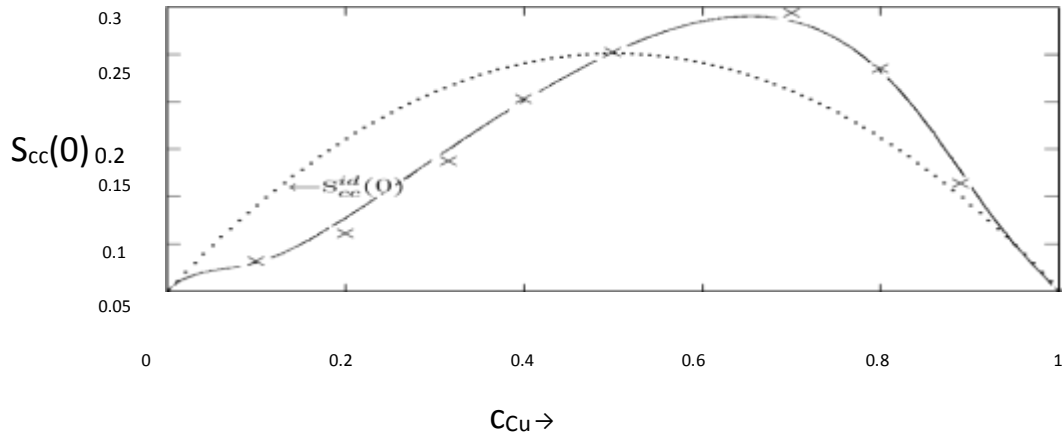


Fig. 2.7. Concentration fluctuations in the long wavelength limit  $S_{cc}(0)$  and  $S_{cc}^{id}(0)$  versus concentration for Cu–In liquid alloys at 1073 K. The solid line denotes theoretical values while the cross denotes experimental data, respectively. The dot denotes the ideal values  $S_{cc}^{id}(0)$  (Odusote., 2008).

The complex formation model using Flory’s approximation solution has been used to describe the thermodynamic properties of some liquid binary alloys with more emphasis on Gibbs free energy of mixing, concentration-concentration fluctuation and Warren-Cowley short-range order parameter in this review, and the same model will be used for investigating the thermodynamic properties of liquid binary alloys under consideration in Chapter 3.

## CHAPTER THREE

### METHODOLOGY

#### 3.1 Introduction

A complex formation model has been used to investigate the thermodynamic properties of Sb-Sn (Antimony tin), Bi-Sb (Bismuth antimony) and Bi-Sn (Bismuth tin) at temperatures 1873K, 905K, 1200K and 600K respectively. In this model, CFM formalism has been applied to Sb-Sn, Bi-Sb and Bi-Sn compound forming alloy to describe the behavior of their mixing properties. Complex Formation Model has its basis on the typical binary liquid alloy which form a compound at one or more stoichiometric composition and therefore behaves like ternary mixture consisting of A atoms, B atoms, and a chemical compound or pseudomolecule  $A_\mu B_\nu$ .

We assume that a binary alloy consists of a pseudo ternary mixture of  $N_A = c$  moles of A atoms and  $N_B = N(1-c)$  moles of B atoms, and a type  $A_\mu B_\nu$  of the chemical complex. Here  $\mu$  and  $\nu$  are assumed to be small integers,  $c$  is the atomic fraction of A atoms and  $N$  is the Avogadro's number. Following the complex formation model Sb-Sn, Bi-Sb and Bi-Sn, and from the phase diagram (Hultgren *et al.* 1963). It follows that it consists of  $n_1$  atoms of Sb,  $n_2$  atoms of Sn and  $n_3$  moles of the complex SbSn (thus  $\mu=1$  and  $\nu=1$ ),  $n_1$  atoms of Bi,  $n_2$  atoms of Sb and  $n_3$  moles of the complex BiSb (thus  $\mu=1$  and  $\nu=1$ ),  $n_1$  atoms of Bi,  $n_2$  atoms of Sn and  $n_3$  moles of the complex BiSn (thus  $\mu=1$  and  $\nu=1$ ). To write down an expression for G on the above basis, using the conservation of atoms, and setting  $N = 1$ . Consider for definiteness, 1g mole of a mixture of A and B atoms, the mole fraction of A atoms is  $c$ . Let at any

instant these exists as  $n_1$  g mole of A atoms,  $n_2$  g mole of B atoms and  $n_3$  g moles of  $A_\mu B_\nu$ , we have from the conservation of atoms

$$n_1 = Nc - \mu n_3, n_2 = (1 - c) - \nu n_3, \quad (3.1)$$

and

$$n = n_1 + n_2 + n_3 = N - (\mu + \nu - 1)n_3.$$

In the equation,  $c$  is taken to be the atomic fraction of Sb and Bi atoms.

It is necessary to compute Gibbs free energy of mixing  $G$  first, by using Eq. (3.2) coupled with  $\Delta G$  as originally formulated in Flory's solution approximation Eq. (3.3). Once the Gibbs free energy of mixing has been fitted, the expression for the Gibbs energy of mixing was then used to provide an equation for the thermodynamic activity, other thermodynamic functions which are related to  $G_M$  through standard thermodynamic relations can then be readily determined.

### 3.2 GIBBS FREE ENERGY OF MIXING $G_M$

Gibbs free energy of mixing of the binary alloy can be expressed as

$$G_M = -n_3 g + \Delta G \quad (3.2)$$

Here  $g$  is the formation energy of the complex and it follows that the first term in the equation represents the lowering of the free energy due to the formation of complexes in the alloy.  $\Delta G$  represents the free energy of mixing of the ternary mixture of fixed  $n_1$ ,  $n_2$  and  $n_3$  whose constituents Sb, Sn, SbSn, Bi, Sb, BiSb and Bi, Sn, BiSn are assumed to be interacting weakly with each other. The strong bonding between the individual elements is taken into account via the formation of the chemical complex. Using  $\Delta G$  as originally formulated in Flory's solution approximation.

$$\Delta G = RT \left[ \sum_{i=1}^2 n_i \ln \left( \frac{n_i}{N} \right) + n_3 \ln \left\{ \frac{(\mu + \nu)n_3}{N} \right\} + \sum_{i < j} \sum \left\{ \left( \frac{n_i n_j}{N} \right) \frac{v_{ij}}{RT} \right\} \right] \quad (3.3)$$

We can express the free energy of mixing by combining Eq. (3.2) and (3.3) as

$$G_M = -n_3g + RT \left[ \sum_{i=1}^2 n_i \ln \left( \frac{n_i}{N} \right) + n_3 \ln \left\{ \frac{(\mu+v)n_3}{N} \right\} + \sum_{i<j} \sum \left\{ \left( \frac{n_i n_j}{N} \right) \frac{v_{ij}}{RT} \right\} \right] \quad (3.4)$$

Table 3.1. Fitted values of the interaction parameters for the liquid Sb-Sn, Bi-Sb and Bi-Sn alloys.

System	g/RT	Temp/K	$v_{12}/RT$	$v_{13}/RT$	$v_{23}/RT$
Bi-Sb	0.10	1200	-0.13	0.16	0.59
Bi-Sn	-3.0	600	0.3	0.8	1.5
Sb-Sn	0.10	905	0.10	0.20	-0.10

Here, R is the molar gas constant, the  $v_{ij}$ 's are the interaction parameters and by definition independent of composition although they may depend on temperature and pressure. The equilibrium value of  $n_3$  at a given temperature and pressure is given by

$$\left( \frac{\partial G_M}{\partial n_3} \right)_{T,P,N,c} = 0 \quad (3.5)$$

From Equation (3.5) and Equation (3.4) the equilibrium values of  $n_3$  was given by solving the equation (3.6) obtained after differentiating Equation (3.4) with respect to  $n_3$  and rearrangement of terms using Equation (3.1).

$$n_1^\mu n_2^\nu = (n_3 N^{\mu+\nu-1}) K' \exp(Z) \quad (3.6) \text{ where}$$

$$K' = K (\mu + \nu) \exp - (\mu + \nu - 1) \quad , \quad K = \exp - \left( \frac{g}{RT} \right) \quad (3.7) \text{ and}$$

$$Z = \frac{-1}{nRT} [(n_1 - \mu n_3)v_{13} + (n_2 - \nu n_3)v_{23} - (\mu n_2 + \nu n_1)v_{12}] \quad (3.8)$$

On eliminating  $n_{1,2}$ , and  $n$  in Eqs. (3.6) to (3.8) from (3.1), Eq. (3.6) is seen to be an equation in the single unknown  $n_3$ . When the solution of Eq. (3.6) for  $n_3$ , and the

corresponding values of  $n_1$ ,  $n_2$ , and  $n$  are substituted into the Eq. (3.4) one obtains the equilibrium free energy of mixing  $G_M$ .

The numerical solution of (3.6) provides equilibrium values of  $n_3$  which can be used to obtain the Gibbs energy from Eq. (3.4). It is obvious from the above equations that in order to compute  $n_3$  or  $G_M$ , one must have knowledge of  $g$  and the interaction parameters  $v_{ij}$ .

The equations required are as stated above. In other to use complex formation model, we fit values of the interaction parameters  $g$  and  $v_{ij}$  in such a way that the values obtained yield the least deviation between the experimental and fitted values of the Gibbs free energy of mixing  $G_M$ . In order to fit ( a Fortran program was written for the fitting) values for the parameter  $g$  and  $v_{ij}$ , we first calculated the value of  $g$  at the

chemical concentration  $c_c = \frac{\mu}{(\mu+v)}$  using as a starting point,  $g \approx -(\mu + v)G_M$ . The energy parameter  $v_{12}$ ,  $v_{13}$ ,  $v_{23}$  were adjusted in order to reproduce as closely as possible the experimentally measured composition-dependence of the Gibbs energy of mixing. From the fittings the values of  $g$  and  $v_{ij}$  obtained for the liquid alloys being investigated are given in Table 3.11. The set of energy parameters given in Table 3.11 is used in Eq. (3.6) to obtain the numerical values of  $n_3$ . The quantities  $n_1$ ,  $n_2$  and were then obtained by substituting  $n_3$  into Eq. (3.1) and thus the chemical complexes.

The numerical values of thermodynamic activity must be obtained as well in order to compute for other thermodynamic properties. Using the general relationship in Eq. (3.9). The expression for the Gibbs energy of mixing was then used to provide an equation for the thermodynamic activity as in Eq. (3.10).

$$RT \ln \alpha_A = \left( \frac{\partial G_M}{\partial N_A} \right)_{T,P,N_B} = \frac{1}{N} \left[ G_M + (1 - C) \left( \frac{\partial G_M}{\partial c} \right)_{T,P,N} \right] \quad (3.9)$$

with  $G_M$  given by equation (3.23) we have

$$\ln \alpha_A = \ln \left( \frac{n_1}{n} \right) + \frac{1}{RT} \left[ \left( \frac{n_2}{n} \right) v_{12} + \left( \frac{n_3}{n} \right) v_{13} - \sum_{i>j} \sum \left( \frac{n_i}{n} \right) \left( \frac{n_j}{n} \right) v_{ij} \right] \quad (3.10)$$

The values of interaction parameters as shown in Table 3.11 are then put in equation (3.10) to calculate the activity for each of the three systems. Having obtained values for Gibbs free energy of mixing and thermodynamic activities, both will be used to calculate the concentration-concentration fluctuation in the long-wavelength so as to determine the nature of ordering in liquid binary alloys under consideration in terms of compound formation and phase segregation.

### 3.3 Concentration- Concentration Fluctuation

An important parameter in studying the nature of ordering in liquid binary alloys is the long-wavelength limit of the concentration-concentration fluctuation  $S_C(0)$ , which has emerged as an important function to understand alloying behavior in terms of compound formation and phase segregation. Since  $S_C(0)$  is thermodynamically related to the free energy of mixing,  $G_M$  and activity,  $\alpha_A$ .  $S_C(0)$  can be computed using the relationship in Eq. (3.11)

$$\begin{aligned} S_{CC}(0) &= \frac{NK_B T}{\left( \frac{\partial^2 G_M}{\partial C^2} \right)_{T,P,N}} = RT \left( \frac{\partial^2 G_M}{\partial C^2} \right)_{T,P,N}^{-1} = (1-C) \alpha_A \left( \frac{\partial \alpha_A}{\partial c} \right)_{T,P,N}^{-1} \\ &= c \alpha_B \left[ \frac{\partial \alpha_B}{\partial (1-c)} \right]_{T,P,N}^{-1} \end{aligned} \quad (3.11)$$

In the above equation  $\alpha_A$  and  $\alpha_B$  are thermodynamic activities of components A and B in the mixture. It may be emphasized that  $\left( \frac{\partial^2 G_M}{\partial C^2} \right)$  is also known as the stability of

the solution. The reciprocal of  $S_C(0)$ , i.e.  $RT/S_{CC}(0)$ , is a measure of the stability of the mixture

Using Eq. (3.11),  $S_C(0)$  can readily be obtained. However, we will use a more reliable expression in Eq. (3.12) for  $S_{CC}(0)$  which involves  $n_i$ , its derivatives with respect to concentration,  $v_{ij}$  and its coordination number  $Z$ ; therefore,

$$S_C(0)^{-1} = \Lambda + Y \quad (3.12)$$

Where

$$\Lambda = \left( \sum_{i=1}^3 \frac{(n_i)^2}{n_i} \right) - \frac{\frac{1}{2}Z\delta^2(n'_3)^2}{\Phi} \quad (3.13)$$

and

$$Y = \frac{2}{\Phi RT} \sum \sum_{i<j} v_{ij} \left( n'_i n'_j + \frac{\partial n'_3 (n'_i n'_j + n_i n'_j)}{\Phi} \right) + \frac{\partial^2 (n'_3)^2 n_i n_j}{\Phi} \quad (3.14)$$

The prime on the n's refers to their first derivative with respect to  $c$  while values of  $\partial = \frac{2(\mu+\nu-1)}{z}$  and  $\Phi = 1 - \delta n_3$  were used in the above equation. We observe that the Flory approximation for  $S_{CC}(0)$  (which is the approximation we have used to express  $G_M$ ) can be obtained simply by setting  $Z = \infty$  in the expression above. This implies that once the Gibbs energy of mixing has been fitted, all the parameters required for the calculation of  $S_C(0)$  must have to be determined and are expected to be kept constant during the course of the calculations. In the present calculation, we have used the typical  $Z = 12$  for our calculations.

It is important to say that the values of  $S_{CC}(0)$  is very difficult and complex to obtain experimentally so  $S_{CC}(0)$  experimental value can be obtained directly from the activity data with the aid of the equation (3.11)

The  $S_C(0)$  values obtained by numerical differentiation of the experimental activity data taken from selected thermodynamic (Hultgren, *et al* 1963) using equation (3.11) are usually referred to as experimental  $S_{CC}(0)$  in literature. Having obtain values for

$S_c(0)$ , it is very important to have an insight into the nature of the local arrangement of atoms in the mixture (for liquid alloys under consideration), which will be calculated using Warren-Cowley's short-range order parameter.

### 3.3 Warren-Cowley Short Range Order Parameter

The degree of order and segregation in the liquid alloy can be quantified by another important function, known as the Warren-Cowley short-range order parameter. The knowledge of  $\alpha_1$  which has been computed for all the alloys provides immediate insight into the local arrangement of atoms in the mixture.  $\alpha_1 = 0$  corresponds to a random distribution of atoms,  $\alpha_1 < 0$  refers to unlike atoms pairing as nearest neighbour, whereas  $\alpha_1 > 0$  corresponds to a situation in which like atoms pair in the first coordination shell. For nearest neighbor sites, it can be defined as

$$\alpha_1 = 1 - \frac{P_{AB}}{(1-c)} \quad (3.15)$$

Where  $P_{AB}$  is the conditional probability of finding B-atom next to a given A-atom. In terms of the bond between unlike atoms Eq. (19) can be expressed as

$$\alpha_1 = \frac{S-1}{S(Z-1)+1}, \quad ; \quad S = \frac{S_{CC}(0)}{c(1-c)} \quad (3.16)$$

$z$  being the coordination number of the alloy. For the present calculation,  $z$  is taken as 12 and the  $S_c(0)$  values are as obtained from equation (3.12). For the present calculation, Eq. (3.16) was used to determine the values for Warren-Cowley's shortrange order parameter. With the values obtained, we can determine the position of the atoms' arrangement in the mixture if the value is minimum ( $\alpha_1^{min} = -1$ , implying a complete ordering of unlike atoms as the nearest neighbor) or maximum ( $\alpha_1^{max} = 1$  implies total segregation leading to phase separation). After determining

the local ordering, enthalpy and entropy will only be discussed, so as to determine if interaction parameters are temperature dependent or not.

### 3.4 Enthalpy and entropy of mixing

Within the complex formation model, the evaluation of enthalpy of mixing is very important because it gives an indication of the temperature dependence of the interaction parameters. The enthalpy of formation  $H_M$  was obtained from the standard thermodynamic expression in Eq. (3.19)

$$H_M = G_M - T \left( \frac{\partial G_M}{\partial T} \right)_P \quad (3.19)$$

From the expression of  $G_M$  in Eq. (3.4), we have

$$H_M = -n_3 g + n_3 T \left( \frac{\partial g}{\partial T} \right)_P + \sum_{i < j} \sum \left( \frac{n_i n_j}{N} \right) \left[ v_{ij} - T \left( \frac{\partial v_{ij}}{\partial T} \right)_P \right] \quad (3.20)$$

and the entropy of mixing

$$S_M = \frac{H_M - G_M}{T} \quad (3.21)$$

Gives

$$S_M = -n \left( \frac{\partial g}{\partial T} \right)_P - R [n_1 \ln n_1 + n_2 \ln n_2 + n_3 \ln \{(\mu + v)n_3\}] - \sum_{i < j} \sum n_i n_j \left( \frac{\partial v_{ij}}{\partial T} \right)_P \quad (3.22)$$

Equation (3.20) and (3.22) have been used to evaluate  $H_M$  and  $S_M$  respectively, their temperature derivatives  $\frac{\partial g}{\partial T}$  and  $\frac{\partial v_{ij}}{\partial T}$  are ascertained by using the observed values of  $H_M$  in Eq. (3.20). Our interest is to find out what happens when the temperature dependence of the interaction parameter was neglected i.e.  $\frac{dv}{dT} = 0$  and both  $H_M$  and  $S_M$  computed, and when the temperature dependence of the interaction parameters are involved in the computation.

## CHAPTER FOUR

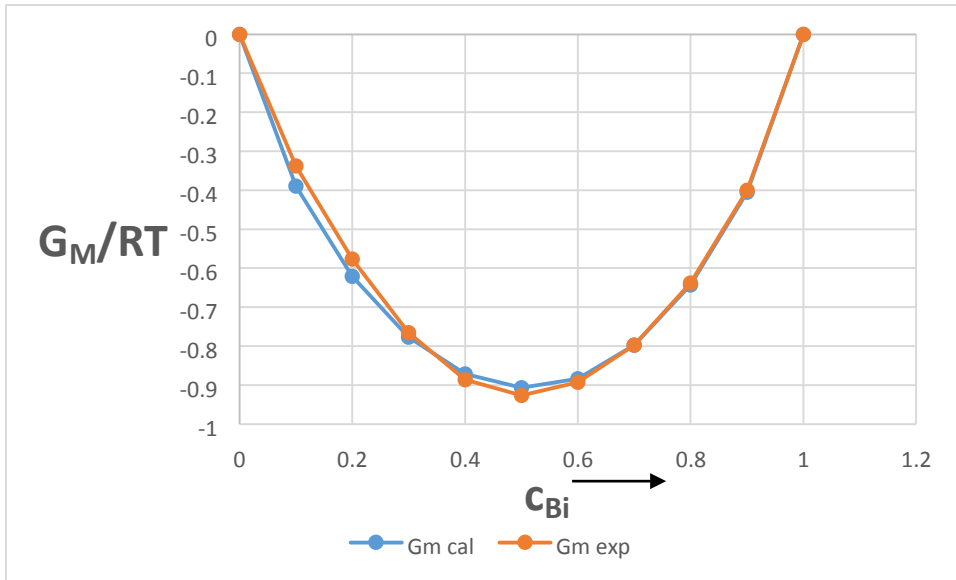
### RESULTS AND DISCUSSION

#### 4.1 Gibbs free energy of mixing

The fitted values of the interaction parameters for the three systems, Sb-Sn, Bi-Sb, and Bi-Sn are quite good at the temperature of interest (Fig. 4.1) because the fitted and experimental values of the free energy of mixing of the liquid alloys compare well with each other. From the point of view of the interaction parameters, that is,  $v_{ij}$  and  $g/RT$ , the latter is the most physically meaningful since it is a measure of the formation of a complex in each alloy. Although the value of  $g/RT$  from Table 4.1 in two of the liquid system considered namely Bi-Sb and Sb-Sn is positive but less than one at the temperature of observation. It is quite obvious that the values are very low compared with 16.7 for Mg-Bi and 10.84 for Tl-Te and 47.8 for K-Te respectively (Bhatia and Hargrove.,1974) 2.8 for Te-Ga and 3.1 for Te-Tl liquid alloys (Awe et al., 2003). Therefore the two liquid alloys do not have a strong tendency to form complexes, in other words, it indicates that Sb-Sn and Bi-Sb are weakly interacting systems. While the value of  $g/RT$  for Bi-Sn is negative and less than one, negative  $g/RT$  signifies poor interaction and therefore Bi-Sn alloy is a poor interacting system.

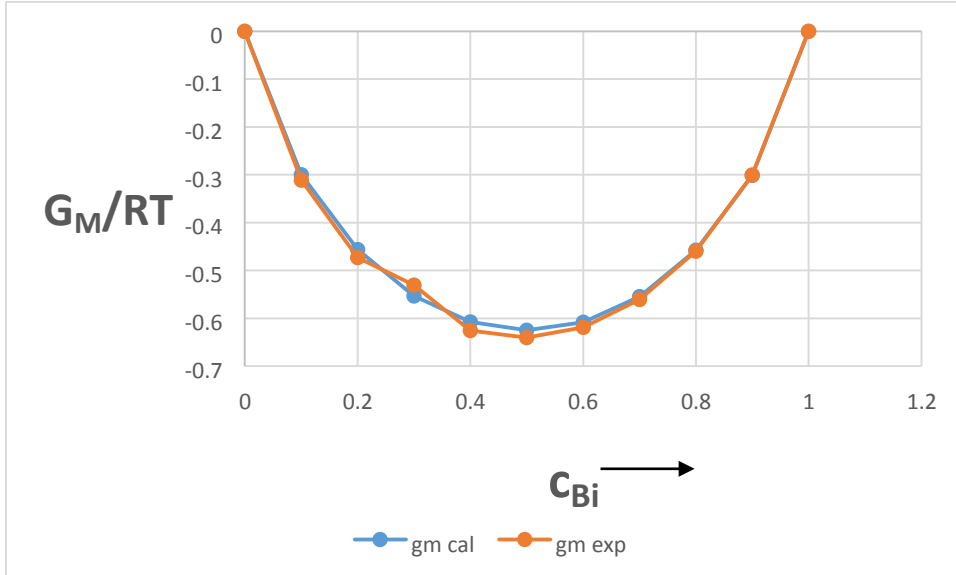
Table 4.1. Fitted values of the interaction parameters for the liquid Sb-Sn, Bi-Sb and Bi-Sn alloys.

System	$g/RT$	Temp/K	$w_{12}/RT$	$w_{13}/RT$	$w_{23}/RT$
Bi-Sb	0.10	1200	-0.13	0.16	0.59
Bi-Sn	-3.0	600	0.3	0.8	1.5
Sb-Sn	0.10	905	0.10	0.20	-0.10



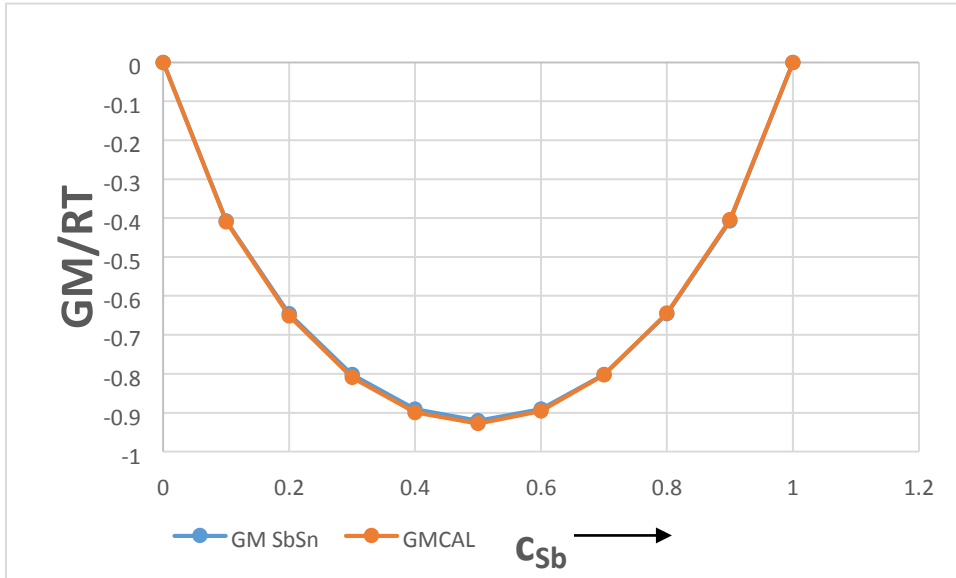
Bi-Sb

Fig. 4.1 Concentration-dependence of  $G_M/RT$  for Bi-Sb liquid alloys at 1200K. The Blue solid line denotes theoretical values while the pink solid line denotes experimental data, respectively.



Bi-Sn

Fig. 4.2 Concentration-dependence of  $G_M/RT$  for Bi-Sn liquid alloys at 600K. The Blue solid line denotes theoretical values while the pink solid line denotes experimental data, respectively.



### Sb-Sn

Fig. 4.3 Concentration-dependence of  $G_M/RT$  for Sb-Sn liquid alloys at 905K. The Blue solid line denotes theoretical values while the pink solid line denotes experimental data, respectively.

For a strong interaction between the constituent elements the Gibbs free energy of mixing  $\frac{G_M}{RT} \leq -3$ , the maximum value for Gibbs free energy of mixing for both Bi-Sb and Sb-Sn in Fig. 4.1 and 4.3 are -0.907 at  $c = 0.5$  and -0.926 at  $c = 0.5$  respectively, this shows that the two liquid alloys are the weakly interacting system, while Bi-Sn is -0.640 at  $c = 0.5$  is a weaker interacting system than both Bi-Sb and Sb-Sn alloys.

With regards to other interaction parameters,  $v_{12}$ ,  $v_{13}$ ,  $v_{23}$  one can explain their physical meaning using a scheme in which the subscript 1 represents the A atoms, 2 represents B atoms and 3 represents the complex  $A_\mu B_\nu$ . It follows from this that  $v_{12}$  is a measure of the interaction between A and B atoms. Thus, a value greater than zero indicates an alloy that exhibits hetero-coordinated at certain compositions, while a value less than one is evidence of a homo-coordinated system. This is evident from Table 4.1, for Bi-Sb, Bi-Sn, and Sb-Sn system.

#### 4.2 Concentration-Fluctuation

In figure 4.4 and 4.6 it is noted that  $S_{CC}(0) \ll S_{CC}^{id}(0)$  i.e., computed values are less than the ideal values at all compositions range in the two systems. The implication of this is that Bi-Sb, and Sb-Sn alloys are compound forming over the composition range. This indicates the tendency of hetero-coordination, i.e., unlike atoms of BiSb, and Sb-Sn pairing as the nearest neighbour. Compare with  $S_C(0)$  in Cu-In where the liquid alloys undergo a transformation from an ordered state (compound formation) to a segregated state (Odusote., 2008), but behave in a similar way to compound forming Al-Fe alloy, where  $S_{CC}(0) \ll S_{CC}^{id}(0)$ .

However, in Fig. 4.5.  $S_{CC}(0) \gg S_{CC}^{id}(0)$  i.e., the computed value is greater than the ideal value at all compositions in Bi-Sn alloy. This indicates a tendency for homocoordination and leads to phase segregation (preference for like atoms to pair as the nearest neighbor).

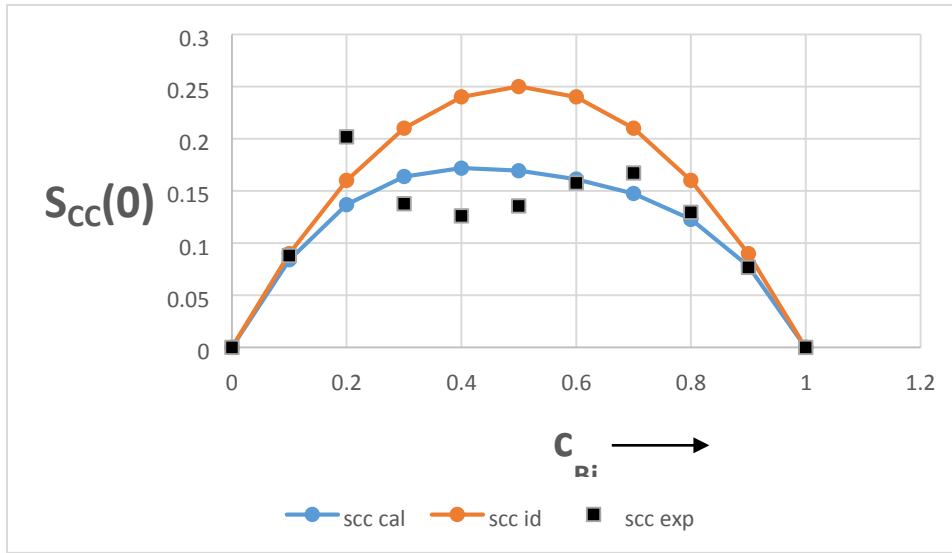


Fig. 4.4 Concentration-concentration fluctuations,  $S_C(0)$  versus composition for Bi-Sb liquid alloys at 1200K. The Blue solid line denotes ideal values while the pink solid line denotes theoretical values, rectangle symbol represents experimental value respectively.  $C_{Bi}$  is the concentration of Bismuth in the alloy.

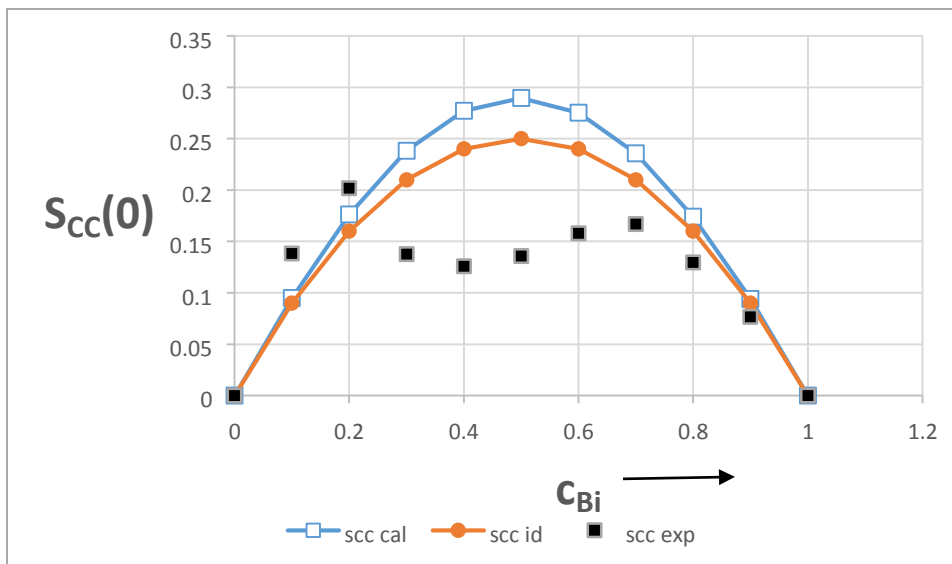


Fig. 4.5 Concentration-concentration fluctuations,  $S_C(0)$  versus composition for Bi-Sn liquid alloys at 600K. The Blue solid line denotes Ideal values while the pink solid line denotes theoretical values, rectangle symbol represents experimental value respectively.  $C_{Bi}$  is the concentration of Bismuth in the alloy.

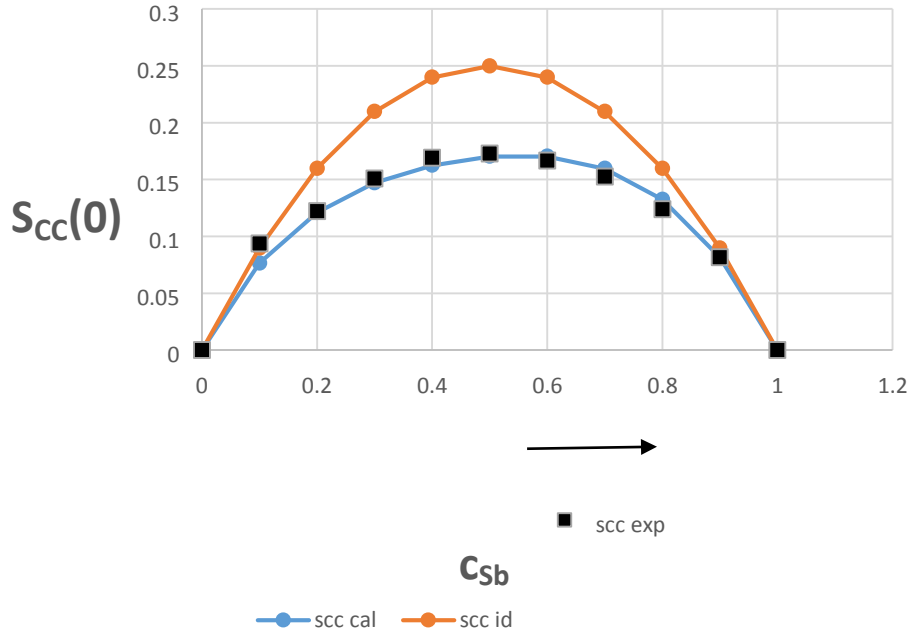


Fig. 4.6 Concentration-concentration fluctuations,  $S_C(0)$  versus composition for SbSn liquid alloys at 905K. The Blue solid line denotes Ideal values while the pink solid line denotes theoretical values, rectangle symbol represents experimental value respectively.  $c_{Sb}$  is the concentration of Bismuth in the alloy.

The graph from Fig. 4.4 showed that  $S_C(0)$  exhibits a maximum value of 0.171 at  $c = 0.4$  which means it is not symmetry at  $c = 0.5$ , this implies a tendency towards clustering and indicates a weakly pronounced hetero-coordination. While the plot from Fig. 4.5 showed that  $S_C(0)$  exhibits a maximum value of 0.289 at  $c = 0.5$  and greater than the maximum value for  $S_{cc}^{id}(0)$ , therefore indicate a tendency towards segregation, leading to a phase separation with a pronounced homo-coordination. Also the graph from Fig. 4.6 showed that  $S_C(0)$  exhibits a maximum value of 0.1727 at  $c = 0.5$ , and implies a tendency towards clustering which indicates a weakly pronounced hetero-coordination

### 4.3 Short-Range Order Parameter

It is noted in figure 4.7 and 4.9 that the values of  $\alpha_1$  for both Bi-Sb and Sb-Sn alloys are negative. The implication of the negative values of  $\alpha_1$  is that both alloys are hetero-coordinated, while according to figure 4.8 the value of  $\alpha_1$  for Bi-Sn alloy being positive indicates phase segregation (homo-coordination).

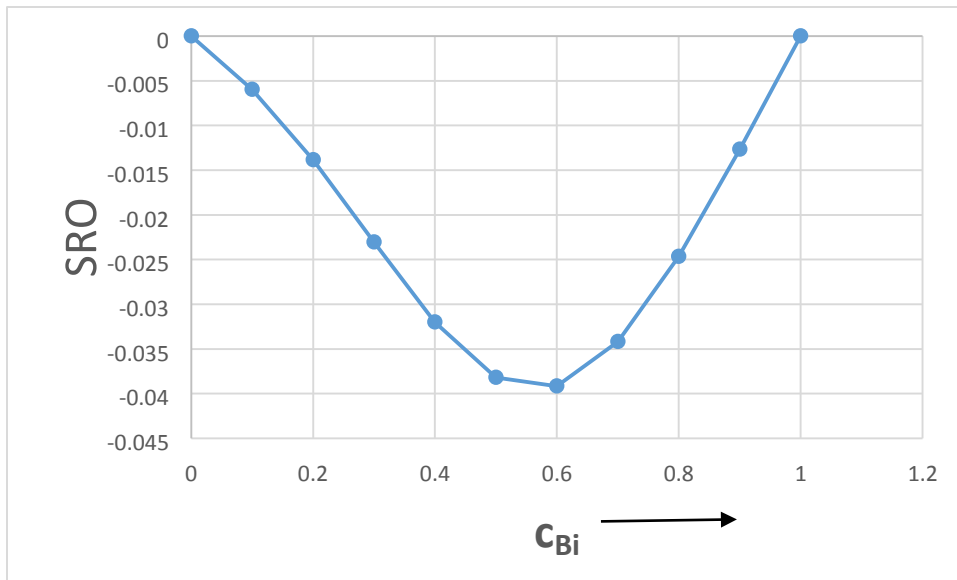


Fig. 4.7 Calculated Warren-Cowley short-range order parameter,  $\alpha_1$  versus concentration for Bi-Sb liquid alloys at 1200K.

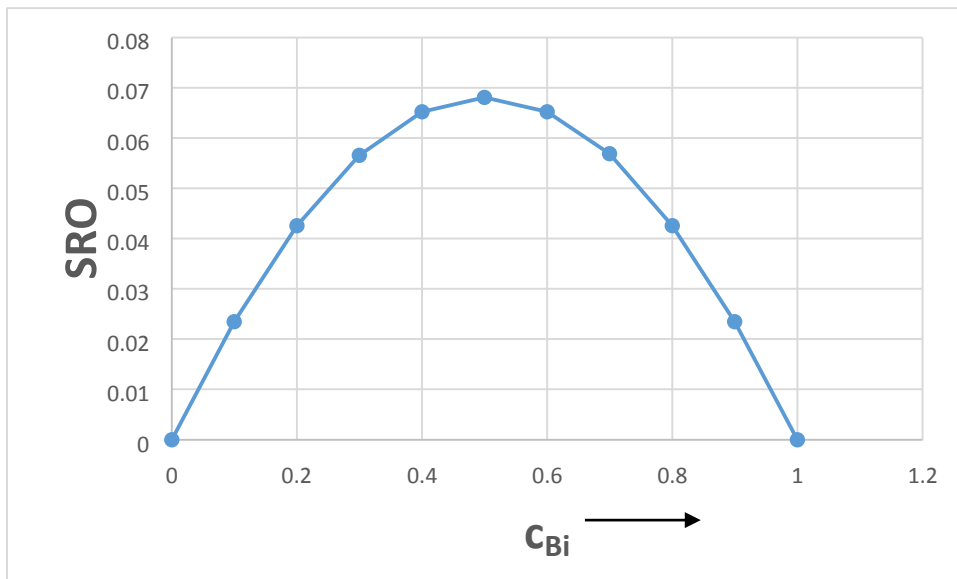


Fig. 4.8 Calculated Warren-Cowley short-range order parameter,  $\alpha_1$  versus concentration for Bi-Sn liquid alloys at 600K

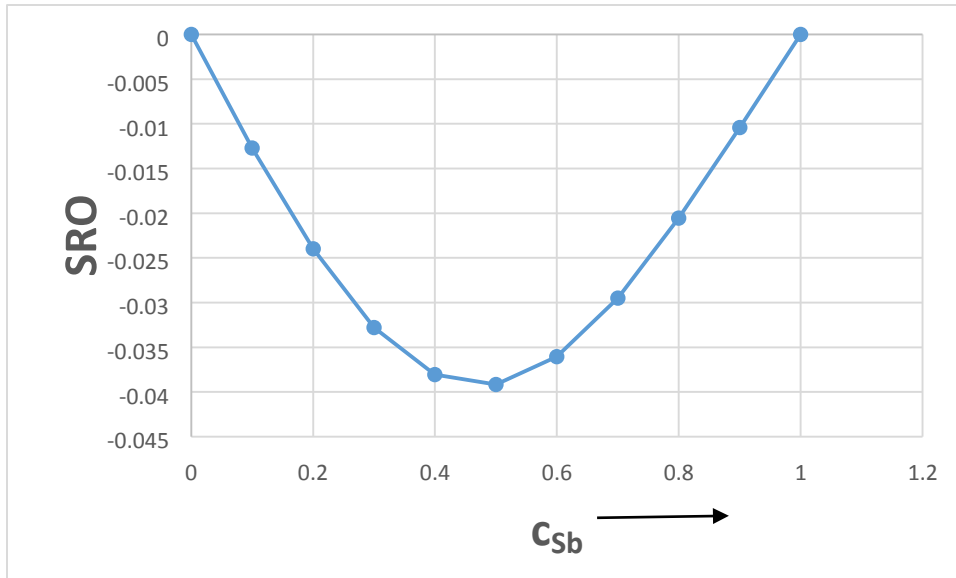


Fig. 4.9 Calculated Warren-Cowley short-range order parameter,  $\alpha_1$  versus concentration for Sb-Sn liquid alloys at 905K.

It is noted from Fig. 4.7, the values of  $\alpha_1$  for Bi-Sb alloys are negative. This can be seen from the plot of Warren-Cowley's short-range order in Fig. 4.7 the plot showed that Bi-Sb exhibited a minimum value of  $\alpha_1$  as  $\alpha_1^{min} = -0.0391$ . These values are quite small compared to the value of  $\alpha_1$  for complete order which is  $\alpha_1^{min} = -1.0$ . The implication of the negative values of  $\alpha_1$  is that liquid Bi-Sb alloy local ordering is very weak. While from the values of  $\alpha_1$  for liquid Bi-Sn alloy are positive which means that liquid Bi-Sn alloy exhibits complete dis-ordering. This can be seen from the plot of Warren-Cowley's short-range order in Fig. 4.8. The graph showed that Bi-Sn exhibited a maximum value of  $\alpha_1$  as  $\alpha_1^{max} = 0.0680$ . These values are quite big compared to the value of  $\alpha_1$  for complete order which is  $\alpha_1^{min} = -1.0$ . Also from

Fig. 4.9 the values of  $\alpha_1$  for liquid Sb-Sn alloy are negative and Sb-Sn exhibited a minimum value of  $\alpha_1$  as  $\alpha_1^{min} = -0.039$ . These values are quite small compared to the value of  $\alpha_1$  for complete order which is  $\alpha_1^{min} = -1.0$ .

Compare to Te-Ga where  $\alpha_1$  for Te-Ga shows that within the concentration range  $0.0 \leq C_{Te} \leq 0.480$  Te-Ga is weakly ordered because  $\alpha_1 < 0$ . Also  $\alpha_1$  of Te-Ga shows that within the remaining range of concentration (i.e  $0.480 \leq C_{Te} \leq 1.0$  ) it is chemically ordered while Te-Tl exhibit compound forming throughout the composition range (Awe et al., 2003).

#### 4.4 Enthalpy and entropy of mixing

The heat enthalpy and entropy of mixing are two important parts of a thermodynamic function that can be used to dictate the degree of segregation in liquid binary alloys. Equation 3.42 and 3.44 has been used to evaluate  $H_M$  and  $S_M$  respectively. The temperature and energy parameters (Table 4.2) are the same.

Table 4.2. Fitted values for temperature derivatives interaction parameters for the Sb-Sn, Bi-Sb, and Bi-Sn liquid alloys.

System	$\frac{\partial g}{\partial T}$	Temp/K	$\frac{\partial v_{12}}{\partial T}$	$\frac{\partial v_{13}}{\partial T}$	$\frac{\partial v_{23}}{\partial T}$
Bi-Sb	0.4	1200	-0.04	0.01	0.25
Bi-Sn	-6.0	600	0.02	0.01	0.02
Sb-Sn	1.2	905	-0.92	0.75	1.4

Computed values of  $H_M$  along with the experimental values are presented in figures 4.10, 4.11 and 4.12 respectively as a function of concentration. The plot shows a good agreement between the experimental and computed values of  $H_M$ . Also, the enthalpy of mixing for Bi-Sb liquid alloy is positive at all concentration and the contribution from the formation of complexes is maximum when the value is 0.0581 at  $c = 0.5$ . The enthalpy of mixing for Bi-Sn liquid alloy is positive at all concentrations and symmetry at equiatomic composition, the contribution from the formation of complexes is maximum when the value is 0.05810 at  $c = 0.5$ . While the enthalpy of mixing for Sb-Sn liquid alloy is negative at all concentration and asymmetry at equiatomic composition, the contribution from the formation of complexes is minimum when the value is -0.1897 at  $c = 0.6$  and a slight deviation in the concentration range  $0.1 \leq c_{Sb} \leq 0.7$ .

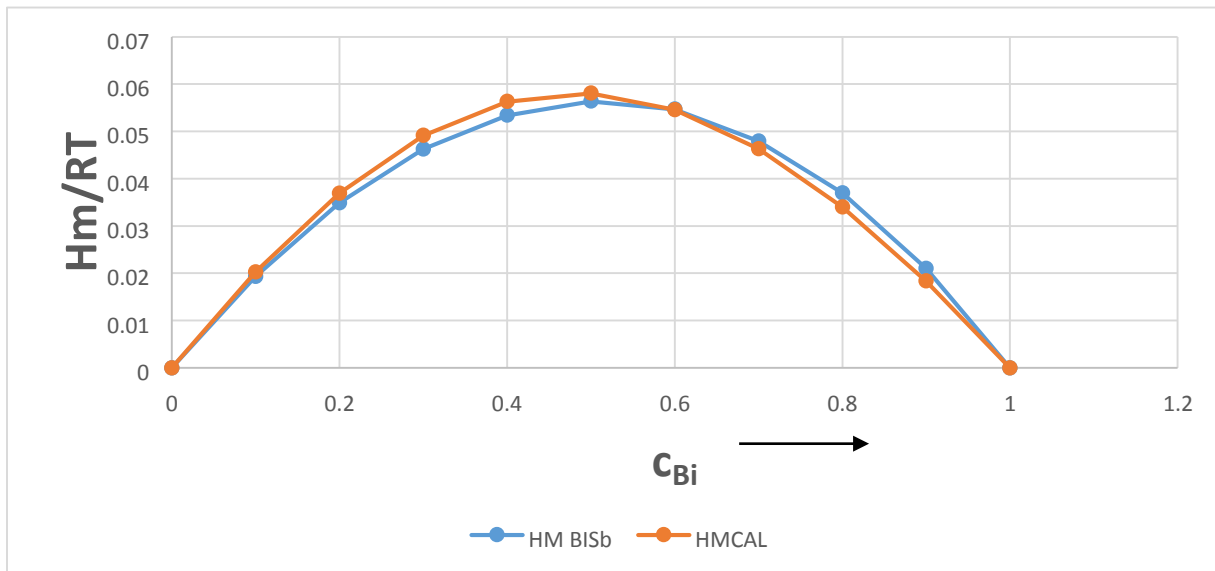


Fig. 4.10 Enthalpy of mixing  $\frac{H_M}{RT}$  versus concentration in Bi-Sb liquid alloys at 1200K. The Blue solid lines denote experimental values while the pink solid denoted theoretical values. The experimental data are from Ref. 23.

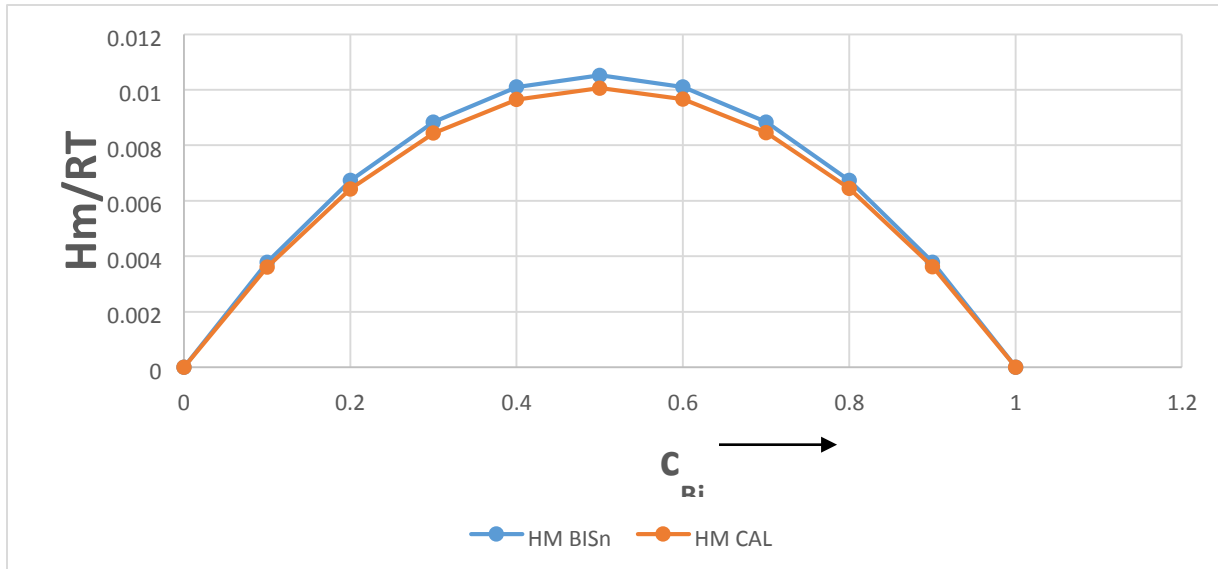


Fig. 4.11 Enthalpy of mixing:  $\frac{H_M}{RT}$  versus concentration in Bi-Sn liquid alloys at 600K. The Blue solid lines denote experimental values while the pink solid denoted theoretical values. The experimental data are from Ref. 23.

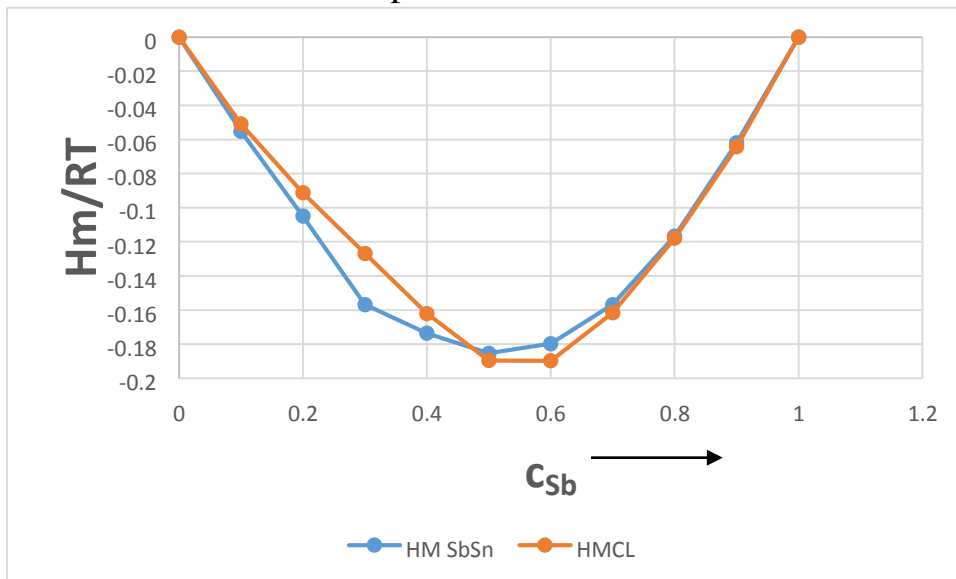


Fig. 4.12. Enthalpy of mixing:  $\frac{H_M}{RT}$  versus concentration in Sb-Sn liquid alloys at 905K. The Blue solid lines denote experimental values while the pink solid denoted theoretical values. The experimental data are from Ref. 23.

Computed values of  $S_M$  along with the experimental values are presented in figures 4.13, 4.14 and 4.15 respectively as a function of concentration. The plot shows that they are all symmetries at equiatomic composition ( $c = 0.5$ ) and there is a good

agreement between the experimental and computed values of  $S_M$ , except a slight deviation at the concentration range  $0.2 \leq c_{Sb} \leq 0.9$ . in figure 4.15, this discrepancy may be caused due to the formation of more than one complexes which is not covered in our analysis. The entropy of mixing for Bi-Sb liquid alloy is positive at all concentration and the contribution from the formation of complexes is maximum when the value is 0.981 at  $c = 0.5$ , the observed values are symmetrical around  $c = 0.5$ . Also, the entropy of mixing for Bi-Sn (figures 4.14) liquid alloy is positive at all concentrations and the contribution from the formation of complexes is maximum when the value is 0.6990 at  $c = 0.5$ . While the entropy of mixing for Sb-Sn liquid alloy is positive at all concentrations and the contribution from the formation of complexes is maximum when the value is 0.8840 at  $c = 0.5$ .

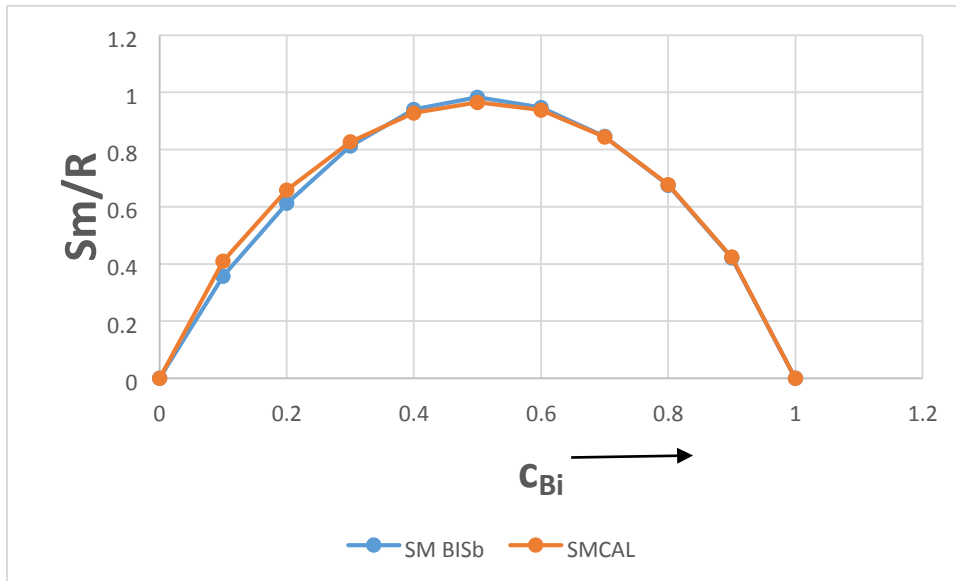


Fig. 4.13 Entropy of mixing:  $\frac{S_M}{R}$  versus concentration in Bi-Sb liquid alloys at 1200K. The Blue solid line denotes experimental values while the pink solid line denotes theoretical value.

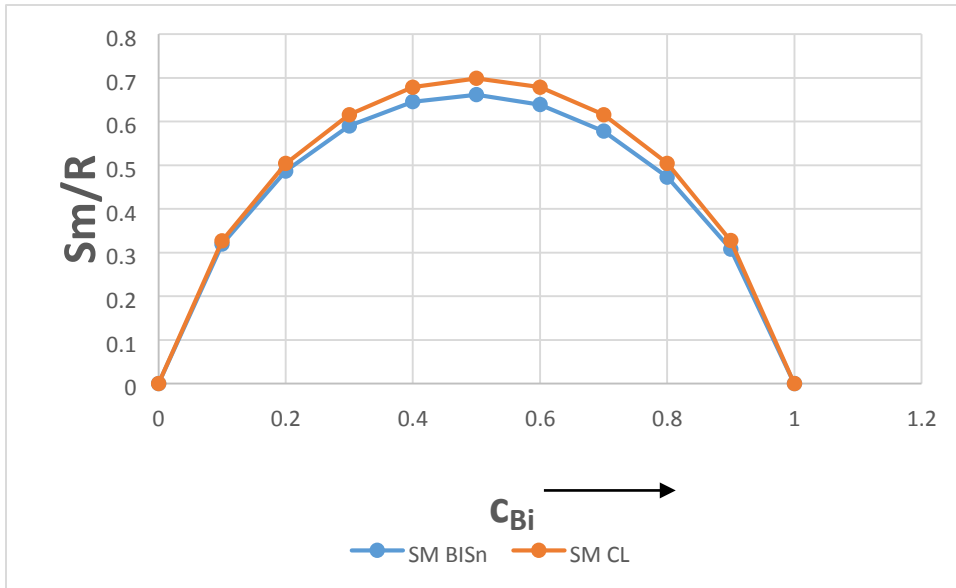


Fig. 4.14 Entropy of mixing:  $\frac{S_M}{R}$  as a function of concentration in Bi-Sn liquid alloys at 600K. The Blue solid line denotes experimental values while the pink solid line denotes theoretical values.

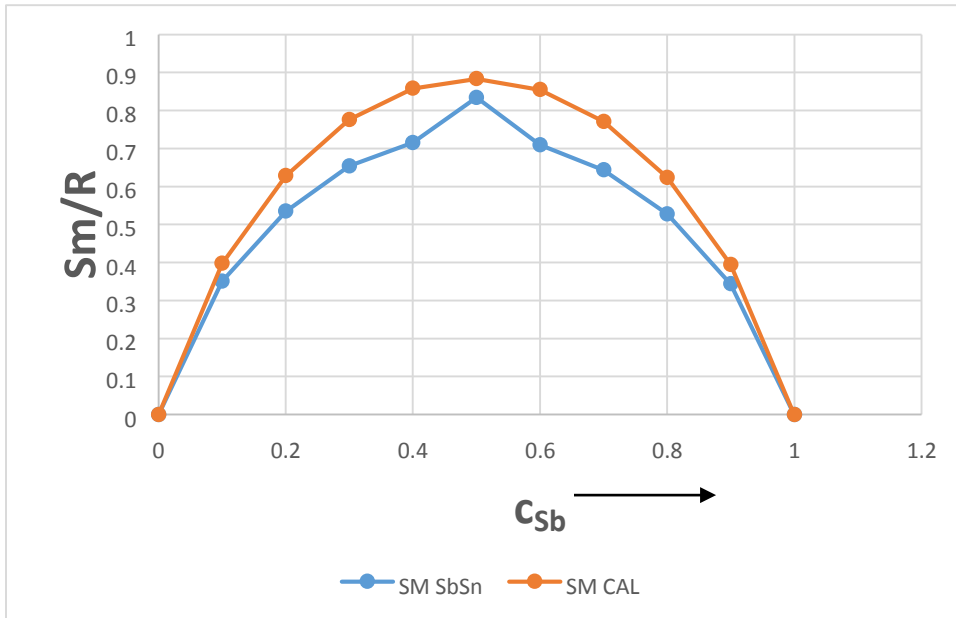


Fig. 4.15. The entropy of mixing:  $\frac{S_M}{R}$  as a function of concentration in Sb-Sn liquid alloys at 905K. The Blue solid lines denote experimental values while the pink solid line denotes theoretical value.

## CHAPTER FIVE

### CONCLUSION

#### 5.1 SUMMARY

The complex formation model has been used to study the thermodynamic properties of Bi-Sb, Bi-Sn, and Sb-Sn binary liquid alloys. The investigation reveals that BiSb and Sb-Sn alloys are weak ordered systems.

Fig. 4.1. Shows that the fitted values of the interaction parameters for the system, Bi-Sb are quite good at the temperature of interest. This is due to the fact that both fitted and experimental values of the free energy of mixing compare well with each other. The values are found to be negative at all concentrations with  $G_{Mmin} = 0.9070RT$  at  $c_{Sb} = 0.5$ . In general,  $\frac{G_M}{RT}$  for a strong interaction in liquid binary alloys, Gibbs free energy mixing is less than or equal to  $-3$  ( $\frac{G_M}{RT} \leq -3$ ). This justifies the conclusion that Bi-Sb alloy has no strong tendency to form complexes, in other words, Bi-Sb is weak interacting systems. In Fig. 4.4 it is noted that  $S_C(0) \ll S_{CC}^{id}(0)$ , i.e., the computed value is less than the ideal values at all compositions in all the systems. The implication of this is that Bi-Sb alloy form compound over all the composition range and indicates a tendency for hetero-coordination, i.e., unlike atoms of Bi-Sb pairing as the nearest neighbor and implies a tendency towards clustering and a weakly pronounced hetero-coordination. This can be seen in Fig.

4.4, the graph showed that  $S_C(0)$  exhibits a maximum value of 0.1718 at  $C = 0.4$ . It is noted from Fig. 4.7 also that the values of  $\alpha_1$  for Bi-Sb alloys are negative. The implication of the negative values of  $\alpha_1$  is that Bi-Sb alloys are hetero-coordinated. The graph shows that Bi-Sb exhibited a minimum value of  $\alpha_1$  as  $\alpha_1^{min} = -0.0391$ , this value is quite small compared to the value of  $\alpha_1$  for complete order which is  $\alpha_1^{min} = -1.0$ .

Also Fig. 4.2 shows that the fitted values of the interaction parameters for the system, Bi-Sn are quite good at the temperature of interest, both fitted and experimental values of the free energy of mixing compare well with each other and the values are found to be negative at all concentrations with  $G_{Mmin} = -0.6253RT$  at  $c_{Bi} = 0.5$ . In Fig. 4.5 it is noted that  $S_C(0) \gg S_{cc}^{id}(0)$ , i.e., computed values is greater than the ideal values at all compositions in all the system. The implication of this is that Bi-Sn alloy does not form compound over the whole composition range and indicates a high tendency towards segregation and a strong pronounced homo-coordination, i.e., like atoms of Bi-Sn pairing as nearest neighbour. Fig. 4.5 shows that  $S_C(0)$  exhibits a maximum value of 2.894 at  $c = 0.5$ . Also, it is noted from Fig. 4.8 that the values of  $\alpha_1$  for Bi-Sn alloy are positive. The implication of the positive values of  $\alpha_1$  is that Bi-Sn alloy undergo complete dis-ordering. This can be seen from the plot of Warren-Cowley's short-range order in Fig. 4.8. The graph showed that Bi-Sn

exhibited a maximum value of  $\alpha_1$  as  $\alpha_1^{min} = 0.0680$  which are quite big compared to the value of  $\alpha_1$  for a complete order which is  $\alpha_1^{min} = -1.0$ , which quite justify that Bi-Sn undergoes segregation and leads to phase separation.

Fig. 4.3 shows that the fitted values of the interaction parameters for the system, SbSn are quite good at the temperature of interest because both fitted and experimental values of the free energy of mixing compare well with each other. The values are found to be negative at all concentrations with  $G_{Mmin} = -0.9266RT$  at  $C_{Sb} = 0.5$  which justifies the conclusion that Sb-Sn alloy has no strong tendency to form complexes. In other words, it indicates that Sb-Sn is a weak interacting system. In Fig. 4.6 it is noted that  $S_{cc}(0) \ll S_{cc}^{id}(0)$ , i.e., computed values are less than the ideal values at all compositions in all the systems. The implication of this is that Sb-Sn alloy is compound forming over the composition range and indicates the tendency of heterocoordination, i.e., unlike atoms of Sb-Sn pairing as nearest neighbor, Fig. 4.6 show that  $S_{cc}(0)$  exhibits a maximum value of 0.1727 at  $C = 0.5$  which implies a tendency towards clustering and indicates a weakly pronounced heterocoordination. It is noted from Fig. 4.9 that the values of  $\alpha_1$  for Sb-Sn alloy are negative. The implication of the negative values of  $\alpha_1$  confirm that Sb-Sn alloys are heterocoordinated. This can be seen from the plot of Warren-Cowley's short-range order in Fig. 4.9. The graph showed that Sb-Sn exhibited a minimum value of  $\alpha_1$  as

$\alpha_1^{min} = -0.039$ . These values are quite small compared to the value of  $\alpha_1$  for complete order which is  $\alpha_1^{min} = -1.0$ .

Most of the compound-forming binary liquid alloys are good glass formers, for example, AlCa, CaMg, MgZn and CuTi (Singh, 1987). These authors have discussed at length the possible correlation among concentration-concentration fluctuation  $S_C(0)$ , the equilibrium phase diagram, the existence of chemical complexes in the liquid state and glass formation. It has been pointed out that in the glass-forming composition range,  $S_C(0)$  attain ideal values: the liquid exhibits the ideal behavior for the composition. In the framework of complex formation model, one infers that the unassociated species (A and B atoms) and the complex ( $A_\mu B_\nu$ ) mix randomly, such random mixing can presumably hinder nucleation and help glass formation, however, the phenomenon of glass formation in liquid alloys is very involved and may depend on many other factors (Singh, 1987). All the alloys considered in this study do not have a tendency for glass formation.

## 5.2 CONCLUSION

A complex formation model using Flory's approximation has been used to study the thermodynamic properties of Bi-Sb, Bi-Sn, and Sb-Sn liquid binary alloys. Our study indicates that at a temperature of 1200k and 905k, Bi-Sb and Sb-Sn alloys are chemically ordered, and by assuming the existence of a complex of the form Bi-Sb and Sb-Sn, we can reproduce the experimental composition dependence of the

thermodynamic properties of liquid binary Bi-Sb and Sb-Sn alloys. The investigation reveals that both liquid Bi-Sb and Sb-Sn alloys are chemically-ordered alloys, while Bi-Sn exhibits a preference for segregation. Bi-Sn alloy is the least interacting liquid alloy of the three alloys investigated. It is therefore concluded that Bi-Sb and Sb-Sn are more preferable out of the three alloys as lead replacement in solder.

### **5.3 RECOMMENDATION**

We thereby recommend Bi-Sb at 1200 K and Sb-Sn 905 K as a substitute solder and as a replacement for lead in high-temperature solder alloys application. The investigation also revealed that we cannot depend on the interaction energy and the free Gibb's energy of mixing of the liquid alloys alone so as to determine the compound forming alloys and the ordering. We thereby recommend that in selecting the compound forming alloy to work on, the ordering phenomenon should be determined in terms of concentration-concentration fluctuation and Warren-Cowley short-range order parameter.

### **5.4 SUGGESTION FOR FURTHER WORK**

The liquid binary alloys selected for this investigation can further be extended to the ternary system, where surface properties (surface tension and surface segregation) and transport properties (diffusivity and viscosity) can be investigated.

## 5.5 CONTRIBUTION TO KNOWLEDGE

To the best of my knowledge, this is the first time the Complex Formation Model has been used to determine thermodynamic properties of liquid alloys selected.

Flory's approximation was used rather than conformal approximation because (a)

The effect of the difference in size  $A$ ,  $B$  and  $A_{\mu}B_{\nu}$  of the various constituents in the mixture has been taken into consideration and not ignored as in the conformal approximation approach and (b) differences in the interaction parameters between different constituents are not zero contrary to conformal approximation. The Flory's approximation approach is more accurate in the investigation and determining the thermodynamic properties of liquid alloys, which makes it an approximation to a truly complex situation.

## REFERENCES

- Adhikari, D., Singh, B. P., & Jha, I. S. (2011). Concentration Fluctuation in Long Wavelength Limit in Liquid Magnesium Alloy. *The Himalayan Physics*, 2, 47–49.
- Akinlade, O., Singh, R. N., & Sommer, F. (2000). Thermodynamics of liquid Al-Fe alloys. *Journal of Alloys and Compounds*, 299(1–2), 163–168. [https://doi.org/10.1016/S0925-8388\(99\)00682-9](https://doi.org/10.1016/S0925-8388(99)00682-9)
- Anusionwu, B. C. (2006). Thermodynamic and surface properties of Sb-Sn and InSn liquid alloys. *Pramana - Journal of Physics*, 67(2), 319–330. <https://doi.org/10.1007/s12043-006-0076-z>
- Arzpeyma, G., Gheribi, A. E., & Medraj, M. (2013). On the prediction of Gibbs free energy of mixing of binary liquid alloys. *The Journal of Chemical Thermodynamics*, 57(February 2013), 82–91. <https://doi.org/10.1016/j.jct.2012.07.020>
- Asryan, N., & Mikula, A. (2004). Thermodynamic properties of liquid Bi – Sn alloys, 95, 132–135.
- Awe, O. E., Akinlade, O., & Hussain, L. A. (2003). Thermodynamic properties of liquid Te-Ga and Te-Tl alloys. *Journal of Alloys and Compounds*, 361(1–2), 227–233. [https://doi.org/10.1016/S0925-8388\(03\)00451-1](https://doi.org/10.1016/S0925-8388(03)00451-1)
- Bhatia, A.B., Hargrove., W.H and Thorthon, D.E. (1974). Concentration fluctuations and thermodynamic properties of some compounds forming binary molten systems. *Physical Review* 9.
- Bhatia, A.B and Hargrove., W.H (1974). Concentration fluctuations and thermodynamic properties of some compounds forming binary molten systems. *Physical Review B*, 10(8), 3186.
- Chen, C., Lee, B., Chen, H., Wang, C., & Wu, A. T. (2016). Development of New Low Melting Solder Alloys. *IEEE 66th Electronic Components and Technology Conference*, 2–7. <https://doi.org/10.1109/ECTC.2016.14>
- Cowley, J. M. (1950). An approximate theory of order in alloys. *Physical Review*, 77(5), 669–675. <https://doi.org/10.1103/PhysRev.77.669>
- Flory, P. J. (1942). Thermodynamics of high polymer solutions. *The Journal of Chemical Physics*, 10(1), 51–61. <https://doi.org/10.1063/1.1723621>
- Glazer, J. (1995). Metallurgy of low-temperature Pb-free solders for electronic assembly. *International Materials Reviews*, 40(2), 65–93. <https://doi.org/10.1179/095066095790151115>

- Hultgren, R., Orr, R.L., and Anderson, P.D., (1963). Selected Values of Thermodynamic Properties of Metals and alloys {Wiley, New York},. *Fundamentals of Physical Metallurgy.*, 963(10), 3635. Retrieved from <https://babel.hathitrust.org/cgi/pt?id=mdp.39015002061920;view=1up;seq=563>
- Ibrahim, A. M., & Thompson, D. A. (1985). Thermoelectric properties of BiSb alloys. *Materials Chemistry and Physics*, 12(1), 29–36. [https://doi.org/10.1016/0254-0584\(85\)90034-3](https://doi.org/10.1016/0254-0584(85)90034-3)
- Jonsson, B., & Agren, J. (1986). Thermodynamic assessment of Sb-Sn system, 2(September).
- Kulikova, T., Mayorova, A., Shubin, A., Bykov, V., & Shunyaev, K. (2015). Bismuth-indium system : thermodynamic properties of liquid alloys. *Kovove Materialy-Metallic Materials*, 53(3), 133–137. <https://doi.org/10.4149/km2015-3-133>
- Lenoir, B., Dauscher, A., Devaux, X., Martin-Lopez, R., Ravich, Y. I., Scherrer, H., & Scherrer, S. (1996). Bi-Sb alloys: an update. *Fifteenth International Conference on Thermoelectrics.*, 1–36. <https://doi.org/10.1109/ICT.1996.553246>
- Lingley, A. R., Ali, M., Liao, Y., Mirjalili, R., Klonner, M., Sopenan, M., ... Parviz, B. A. (2011). A single-pixel wireless contact lens display. *Journal of Micromechanics and Microengineering*. <https://doi.org/10.1088/09601317/21/12/125014>
- Novakovic, R., Giuranno, D., Ricci, E., Delsante, S., Li, D., & Borzone, G. (2011). Bulk and surface properties of liquid Sb-Sn alloys. *Surface Science*, 605(1–2), 248–255. <https://doi.org/10.1016/j.susc.2010.10.026>
- Odusote, Y. A. (2008). Thermodynamic of Compound Forming Molten Cu-In alloys. *International Journal of Modern Physics B*, (22), 4833–4844.
- Singh, P., Pal, C., & Khanna, K. N. (1985). The entropy of Mixing of Compound Forming Liquid Binary Alloys Using Flory's Formula. *Physics and Chemistry of Liquids*, 14(4), 297–302. <https://doi.org/10.1080/00319108508080992>.
- Singh, R. N. (1987). Short-range order and concentration fluctuations in binary molten alloys. *Canadian Journal of Physics*, 65(3), 309–325. <https://doi.org/10.1139/p87-038>

Singh, R. N., & Sommer, F. (1992). Temperature dependence of the thermodynamic functions of strongly interacting liquid alloys. *Journal of Physics: Condensed Matter*, 4(24), 5345–5358. <https://doi.org/10.1088/0953-8984/4/24/004>

## APPENDIX 1

### Symbols

A,B	-components of a binary A–B alloys
$a_i(i=A,B)$	- activity of component i
$C_i(i=A,B)$	- composition of component i
C,1–C	-composition of components A and B
$C_s,1-C_s$	-surface composition of components A and B
GM	-Gibbs energy of mixing
$X_s$	-excess Gibbs energy of mixing
HM	-enthalpy of mixing
$k_B$	-Boltzman's constant
$\lambda_i(i=A,B)$	- size and shape factor of viscosity of component i
N	-Avogadro's number
R	-gas constant
$S_{cc}(0)$	- concentration fluctuations
$S_{cc}(0, id)$	- concentration fluctuations for the ideal mixing condition
T	-absolute temperature
$V_i(i=A,B)$	- atomic volume of the component i
Z	-coordination number
W	-regular solution energy parameter
$W_{ij}$	-order energy parameters for the CFM
$\alpha_i(i=A,B)$	- surface area of atomic species i
$\alpha_1$	- short-range order parameter

## APPENDIX 2

Calculated values of thermodynamic

Bi-Sb alloy at 1200k

$C_{Bi}$	$G_M/RT$	$S_{cc}(0)$	$\alpha_1$
0.1	-0.38960	0.09000	-0.00596
0.2	-0.62127	0.13694	-0.01383
0.3	-0.77736	0.16367	-0.02304
0.4	-0.87150	0.17181	-0.03201
0.5	-0.90708	0.16931	-0.03819
0.6	-0.88347	0.16118	-0.03914
0.7	-0.79768	0.14739	-0.03418
0.8	-0.63344	0.12276	-0.02465
0.9	-0.40530	0.09000	-0.01268

### APPENDIX 3

Calculated values of thermodynamic

Bi-Sn alloy at 600k

$C_{Bi}$	$G_M/RT$	$S_{cc}(0)$	$\alpha_1$
0.1	-0.18762	0.12491	0.02348mkl
0.2	-0.25584	0.31342	0.04252
0.3	-0.28974	0.58748	0.05657
0.4	-0.30593	0.90353	0.06518
0.5	-0.31071	0.63816	0.06809
0.6	-0.30585	0.90364	0.06519
0.7	-0.28958	0.58759	0.05689
0.8	-0.25561	0.31348	0.04253
0.9	-0.18738	0.12420	0.02348

## APPENDIX 4

Calculated values of thermodynamic		Sb-Sn alloy at 905k	
$C_{Sb}$	$G_M/RT$	$S_{CC}(0)$	$\alpha_1$
0.1	-0.40894	0.09000	-0.01072
0.2	-0.65048	0.12388	-0.02398
0.3	-0.80841	0.14995	-0.03277
0.4	-0.88971	0.16371	-0.03806
0.5	-0.92662	0.16902	-0.03915
0.6	-0.89481	0.16668	-0.03605
0.7	-0.80210	0.15461	-0.02948
0.8	-0.63344	0.12819	-0.02056
0.9	-0.40383	0.09000	-0.01043

## APPENDIX 5

C Program alloy

C name Adedipe Adedayo Mayowa

C Physics Department

C\$debug

C Program for caculating thermodynamic quantities in Flory Approximation.

C Output file 'Flory' contains C, GM, N3, N, ln activity, Scc(0),dn3/dc. C

In the meantime u can enter 0 for dg,dv12,dv13 and dv23.

C Bi-Sn

C dg=-2.125,dv12=-0.12,dv13=-4.78,dv23=0.12

IMPLICIT REAL\*8(A-H,O-Z)

PARAMETER (L=9,NDAT=100)

COMMON /CONCN/ CX,MU,NU,V12,V13,V23,G

COMMON/SK/SAK

DIMENSION YN1(L),YN2(L),YN3(L),YC(L),CM(L),ACVX(L),GMEXP(L)

DIMENSION

HMX(L),SCEP(L),SMX(L),CK(L),CT(L),CN(L),DMDS(L),CR(L)

EXTERNAL FUNC

REAL\*8 MU,NU

EPS=1.d-3

EPS1=1.d-5

OPEN(13,FILE='new11.txt',STATUS='UNKNOWN')

OPEN(12,FILE='new12.txt',STATUS='UNKNOWN')

OPEN(17,FILE='new13.txt',STATUS='UNKNOWN')

OPEN(11,FILE='new14.txt',STATUS='UNKNOWN')

OPEN(5,FILE='new15.txt',STATUS='UNKNOWN')

OPEN(1,FILE='new16.txt',STATUS='UNKNOWN')

OPEN(4,FILE='new17.txt',STATUS='UNKNOWN')

OPEN(14,FILE='new18.txt',STATUS='UNKNOWN')

OPEN(15,FILE='new19.txt',STATUS='UNKNOWN')

OPEN(16,FILE='new23.txt',STATUS='UNKNOWN')

OPEN(21,FILE='bisnactE.txt',STATUS='OLD')

OPEN(6,FILE='bisngmE.txt',STATUS='OLD')

OPEN(7,FILE='bisnfl1.txt',STATUS='OLD')

OPEN(8,FILE='bisnhmE.txt',STATUS='OLD')

OPEN(9,FILE='bisnsmE.txt',STATUS='OLD') MU=1. NU=1.

```

Z=12.0
R=MU
S=NU
C   G=1.5
C   V12=-0.012
C   V13=-0.035
C   V23=0.
    WRITE(*,*) ' input g,v12,v13,v23'
    READ(*,*) g,v12,v13,v23
C   WRITE(*,*) ' input dg,dv12,dv13,dv23'
C   READ(*,*) dg,dv12,dv13,dv23
    DO 20 I=1,9
    READ(21,*) CR(I),ACVX(I)
20  CONTINUE
    DO 2 I=1,9
    READ(6,*) CT(I),GMEXP(I)
C   ACVX(I)=ALOG(ACVX(I))
C2  CONTINUE
    IF (ACVX(I).LE.0.) ACVX(I)=5.D-5
    ACVX(I)=ALOG(ACVX(I))
2   CONTINUE
    DO 172 I=1,9
    READ(7,*) CN(I),SCEP(I)
172 CONTINUE

C   WRITE(13,69) CT(I),HMX(I),ACVX(I),GMEXP(I),SMX(I),SCEP(I)
    DO 173 I=1,9
    READ(8,*) CM(I),HMX(I)
173 CONTINUE

    DO 174 I=1,9
    READ(9,*) CK(I),SMX(I)
174 CONTINUE

C2  CONTINUE
    DO 10 I=1,L

```

```

C   DO 10 I=1,100
      C=0.1*I
C   C=CT(I)
CX=C
DMDS(I)=1.
CCC   DMDS=DMDS(I)
      EN3=ZBRENT(FUNC,0.D0,1.D0,1.D-7)
      IF (EN3.LE.0.) EN3=1.D-10
      EN2=(1.-C)-NU*EN3
      EN1=C-MU*EN3
      IF (EN2.LE.0.) EN2=1.D-10
      IF (EN1.LE.0.) EN1=1.D-10
      EN=EN1+EN2+EN3
      ENX=EN*EN
      GM1=-
EN3*G+EN1*ALOG(EN1)+EN2*ALOG(EN2)+EN3*DLOG((MU+NU)*EN3)
      GM2=EN1*EN2*V12+EN1*EN3*V13+EN2*EN3*V23
      GM=GM1+GM2
      HM=-EN3*(G-DG)+EN1*EN2*(V12-
DV12)+EN1*EN3*(V13DV13)+EN2*EN3*
& (V23-DV23)
      ACV1=DLOG(EN1/EN)+1.+ALOG(EN)-EN+(EN3*V13+EN2*V12)
      ACV2=EN1*EN2*V12+EN1*EN3*V13+EN2*EN3*V23
      ACV=ACV1-ACV2
      ACVA=1.-EN+ALOG(EN2)+EN1*V12-
EN1*EN2*V12EN1*EN3*V13+EN3*V23
& -EN2*EN3*V23
      CX=C+EPS
      Q1=ZBRENT(FUNC,0.D0,1.D0,1.D-7)
      CX=C-EPS
      Q2=ZBRENT(FUNC,0.D0,1.D0,1.D-7)
      DN3=(Q1-Q2)/(2.*EPS)
C   DN3=(q1-en3)/eps
C   WRITE(9,*) C, DN3A, DN3
      DNF=DFRIDR(FUNC,EN3,EPS1,ERR)
C   DN3=DNF

```

$$DN1=1.-MU*DN3$$

$$DN2=-1.-NU*DN3$$

$$DN=DN1+DN2+DN3$$

$$YN1(I)=EN1$$

$$YN2(I)=EN2$$

$$YN3(I)=EN3$$

$$YC(I)=C$$

$$SCC=DN1*DN1/EN1+DN2*DN2/EN2+DN3*DN3/EN3$$

$$SCC=1./SCC$$

$$DD=2.*(DN1*DN1*V12+DN1*DN3*V13+DN2*DN3*V23)$$

$$SCC0=SCC/(1.+DD*SCC)$$

C Z DEPENDENT SCC

$$DAL=2*(R+S-1.)/Z$$

$$D2=DAL*DAL$$

$$PJ=1.-DAL*EN3$$

$$DJ1=V12*(DN1*DN2+DAL*DN3*(DN1*EN2+EN1*DN2))/PJ$$

& +D2\*DN3\*DN3\*EN1\*EN2/PJ/PJ)

$$DJ2=V13*(DN1*DN3+DAL*DN3*(DN1*EN3+EN1*DN3))/PJ$$

& +D2\*DN3\*DN3\*EN1\*EN3/PJ/PJ)

$$DJ3=V23*(DN2*DN3+DAL*DN3*(DN2*EN3+EN2*DN3))/PJ$$

& +D2\*DN3\*DN3\*EN2\*EN3/PJ/PJ)

$$RAP=DN1*DN1/EN1+DN2*DN2/EN2+DN3*DN3/EN3$$

$$RAP1=-0.5*Z*DAL*DAL*DN3*DN3/PJ$$

$$SCCZ=2/PJ*(DJ1+DJ2+DJ3)+RAP+RAP1$$

$$SCCZ=1./SCCZ c$$

THE OTHER ALP1

$$BETA=1.$$

$$YP1=2.*((1.-C)**2*MU+C*C*NU)/(MU+NU)$$

$$YP2=2.*DAL*EN3*(MU-(MU+NU)*C)**2/(PJ*(MU+NU)**2)$$

$$ALP2=(MU+NU-1.)*EN3*(-BETA+YP1+YP2)/(C*(1.-C))$$

$$ALP2=ALP2/Z$$

$$SCC=DN1*DN1/EN1+DN2*DN2/EN2+DN3*DN3/EN3+2.*(DN1*DN2*V12+$$

\$ DN1\*DN3\*V13+DN2\*DN3\*V23)

$$SCC=1./SCC$$

$$SCID=C*(1.-C)$$

```

CB=1.-C
DSCC=SCID-SCCZ
DSCC2=SCID-SCC0
SSW=SCCZ/SCID
ALP1=(SSW-1.)/(SSW*(Z-1.)+1.)
DIFF=1./SSW
DM=SCID/SCCZ
SM=HM-GM
WRITE(11,44) C,HM,HMX(I)
WRITE(1,19) C,DSCC,DSCC2
WRITE(4,69) C,EXP(ACV),EXP(ACVA)
C  WRITE(5,9) C,EXP(ACV),EXP(ACVA)
WRITE(14,46) C,EN1,EN2,EN3,EN
WRITE(12,44) C,GM,GMEXP(I)
WRITE(5,45) C,SM,SMX(I)
WRITE(15,4) C,alp1,DM
C  WRITE(17,24) C,SCCZ,SCID,SCEP(I)
WRITE(13,68) C,ACV,ACVA,ACVX(I)
DEVgmrt=DEVgmrt+ABS(GMEXP(I)-GM)
DEVact=DEVact+ABS(ACVX(I)-ACV1)
C  DEV2=DEV2+ABS(SS(I)-SKD)
DEVsm=DEVsm+ABS(SMX(I)-SM)
DEVhm=DEVhm+ABS(HMX(I)-HM)
DEVscc=DEVscc+ABS(SCEP(I)-SCCZ)
C  WRITE(*,*) C,DEVgmrt,DEVscc
WRITE(*,*) C, DEVsm,DEVhm
END

```